

**UNCLASSIFIED**

NAVAL AIR WARFARE CENTER AIRCRAFT DIVISION  
PATUXENT RIVER, MARYLAND



## TECHNICAL REPORT

REPORT NO: NAWCADPAX--98-8-TR

COPY NO. 20

### FIBER FINISHES FOR IMPROVING GALVANIC RESISTANCE OF IMIDE-BASED COMPOSITES

by

Dr. Ronald E. Allred  
Mr. Richard E. Jensen  
Adherent Technologies, Inc.  
(Contract No. N62269-94-C-1243)

Dr. Thomas A. Donnellan  
Mr. Theotis Williams, Jr.  
Northrop Grumman Corporation  
(Contract No. N62269-94-C-1243)

12 February 1998

Aerospace Materials Division  
Air Vehicle and Crew Systems Technology Department  
Naval Air Warfare Center Aircraft Division  
Patuxent River, Maryland

**DTIC QUALITY INSPECTED 3**

Approved for public release; distribution is unlimited.

**UNCLASSIFIED**


19980415 139

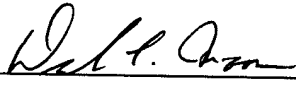
DEPARTMENT OF THE NAVY  
NAVAL AIR WARFARE CENTER AIRCRAFT DIVISION  
PATUXENT RIVER, MARYLAND

NAWCADPAX--98-8-TR  
12 February 1998

The final report on Fiber Finishes for Improving Galvanic Resistance of Imide-Based Composites completed under Contract No. N62269-94-C-1243 is hereby forwarded.

**RELEASED BY:**

 10 Feb 1998  
ROLAND COCHRAN / DATE  
Head, Polymer Composites and Materials Branch

 2/12/98  
DALE MOORE / DATE  
Director, Materials Competency  
Naval Air Warfare Center Aircraft Division

## **REPRODUCTION QUALITY NOTICE**

**This document is the best quality available. The copy furnished to DTIC contained pages that may have the following quality problems:**

- **Pages smaller or larger than normal.**
- **Pages with background color or light colored printing.**
- **Pages with small type or poor printing; and or**
- **Pages with continuous tone material or color photographs.**

**Due to various output media available these conditions may or may not cause poor legibility in the microfiche or hardcopy output you receive.**

**If this block is checked, the copy furnished to DTIC contained pages with color printing, that when reproduced in Black and White, may change detail of the original copy.**

# REPORT DOCUMENTATION PAGE

**Form Approved**  
**OMB No. 0704-0188**

Public reporting burden for this collection of information is estimated to average 1 hour per response, including the time for reviewing instructions, searching existing data sources, gathering and maintaining the data needed, and completing and reviewing the collection of information. Send comments regarding this burden estimate or any other aspect of this collection of information, including suggestions for reducing this burden, to Washington Headquarters Services, Directorate for Information Operations and Reports, 1215 Jefferson Davis Highway, Suite 1204, Arlington, VA 22202-4302, and to the Office of Management and Budget, Paperwork Reduction Project (0704-0188), Washington, DC 20503.

<b>1. AGENCY USE ONLY (Leave Blank)</b>	<b>2. REPORT DATE</b> 12 February 1998	<b>3. REPORT TYPE AND DATES COVERED</b> August 1994 - September 1996	
<b>4. TITLE AND SUBTITLE</b>  Fiber Finishes for Improving Galvanic Resistance of Imide-Based Composites		<b>5. FUNDING NUMBERS</b>	
<b>6. AUTHOR(S)</b>  Dr. Ronald E. Allred Mr. Richard E. Jensen Adherent Technologies, Inc. (Contract No. N62269-94-C-1243)		Dr. Thomas A. Donnellan Mr. Theotis Williams, Jr. Northrup Grumman Corporation (Contract No. N62269-94-C-1243)	
<b>7. PERFORMING ORGANIZATION NAMES(S) AND ADDRESS(ES)</b>  Adherent Technologies, Inc. 11208 Cochiti SE Albuquerque, New Mexico 87123  Northrup Grumman Corporation Advanced Technology Development Center Bethpage, New York 11714		<b>8. PERFORMING ORGANIZATION REPORT NUMBER</b>  NAWCADPAX--98-8-TR	
<b>9. SPONSORING / MONITORING AGENCY NAME(S) AND ADDRESS(ES)</b>  Naval Air Warfare Center Aircraft Division 22347 Cedar Point Road Unit #6 Patuxent River, Maryland 20670-1161		<b>10. SPONSORING / MONITORING AGENCY REPORT NUMBER</b>	
<b>11. SUPPLEMENTARY NOTES</b>			
<b>12a. DISTRIBUTION / AVAILABILITY STATEMENT</b>  Approved for public release; distribution is unlimited.		<b>12b. DISTRIBUTION CODE</b>	
<b>13. ABSTRACT (Maximum 200 words)</b>  The objective of this program is the development and demonstration of galvanic corrosion resistant carbon/BMI composites through the use of reactive finishes to form coatings that isolate the carbon fibers from the BMI matrix. A family of novel reactive coupling agents was formulated into phenolic-based finishes for carbon and graphite fibers that will subsequently react with the fiber and matrix resin during processing to form chemical bonds at the interface and in the interphase. In this process, each fiber is coated uniformly with the phenolic finish and bonded to the finish before the BMI prepregging process. The finish serves to isolate the carbon fibers from the BMI matrix and interrupts the galvanic cell.  The addition of reactive finishes to fiber surfaces serves the dual purposes of protection of the fiber during handling and alteration of the interphase in the cured composite. The surface protection aspect of finishes will become even more critical as composites technology focuses on the use of 3-D braids and weaves for development of low cost composite processes, such as transfer molding. The reactive finish approach will provide a cost efficient means of improving galvanic corrosion resistance in composites with an BMI formulation.			
<b>14. SUBJECT TERMS</b> Fiber Finishes Galvanic Resistance Imide-Based Composites		<b>15. NUMBER OF PAGES</b> 58	<b>16. PRICE CODE</b>
<b>17. SECURITY CLASSIFICATION OF REPORT</b> UNCLASSIFIED	<b>18. SECURITY CLASSIFICATION OF THIS PAGE</b> UNCLASSIFIED	<b>19. SECURITY CLASSIFICATION OF ABSTRACT</b> UNCLASSIFIED	<b>20. LIMITATION OF ABSTRACT</b> SAR

NSN 7540-01-280-5500

Standard Form 298 (Rev. 2-89)  
Prescribed by ANSI Std. Z39-18  
298-102

---

**FIBER FINISHES FOR IMPROVING GALVANIC  
RESISTANCE OF IMIDE-BASED COMPOSITES**

**Final Report  
for the period of August 1994 through September 1996**

**Contract N62269-94-C-1243**

**September 30, 1996**

**prepared by  
Dr. Ronald E. Allred  
Mr. Richard E. Jensen  
Adherent Technologies, Inc.  
11208 Cochiti SE  
Albuquerque, NM 87123**

**and**

**Dr. Thomas A. Donnellan  
Mr. Theotis Williams, Jr.  
Northrop Grumman Corporation  
Advanced Technology Development Center  
Bethpage, NY 11714**

---



# CONTENTS

Executive Summary .....	6
Introduction .....	7
Experimental Procedures .....	10
Materials .....	10
Coupling Agent Synthesis and Characterization .....	10
Finish Formulation Development .....	11
Finish Characterization .....	13
Prepreg Fabrication .....	13
Composite Processing .....	13
Composite Panel Characterization .....	14
Thermal Aging .....	15
Mechanical Testing .....	15
Spectroscopic Characterization .....	15
Galvanic Corrosion Testing .....	16
Electrochemical Impedance Spectroscopy .....	17
Results and Discussion .....	17
Coupling Agent Characterization .....	17
Finish Characterization .....	19
Finish Development .....	24
Composite Screening Tests .....	30
Voltage Contrast XPS .....	30
Galvanic Corrosion .....	31
Electrochemical Impedance Spectroscopy (EIS) .....	44
Composite Mechanical Properties .....	44
Electrochemical Impedance Spectroscopy (EIS) .....	47
Summary and Conclusions .....	50
Acknowledgments .....	51
References .....	51



## FIGURES

Figure 1. Reactive finish interfacial bonding concept.....	9
Figure 2. Schematic chemical structure of reactive coupling agents .....	10
Figure 3. Schematic of finish application apparatus .....	11
Figure 4. Finish processing line .....	12
Figure 5. Composite cure cycle for BMI matrix panels .....	14
Figure 6. Galvanic corrosion sample setup.....	16
Figure 7. Complete set of galvanic corrosion samples.....	16
Figure 8. DSC thermogram at 10°C/min for AT-CA-9306 reactive coupling agent .....	18
Figure 9. DSC thermogram at 10°C/min for neat phenolic resin .....	20
Figure 10. DSC thermogram at 10°C/min for PH9301F finish.....	20
Figure 11. DSC thermogram at 10°C/min for PH9304F finish.....	21
Figure 12. DSC thermogram at 10°C/min for PH9305F finish.....	22
Figure 13. DSC thermogram at 10°C/min for PH9306F finish.....	22
Figure 14. Surface appearance of unsized IM7 fibers.....	25
Figure 15. Appearance of finish with AT-CA-9301 coupling agent.....	26
Figure 16. Appearance of finish with AT-CA-9304 coupling agent.....	27
Figure 17. Appearance of finish with AT-CA-9305 coupling agent.....	28
Figure 18. Appearance of finish with AT-CA-9306 coupling agent.....	29
Figure 19. Fracture surface appearance of unsized IM7/BMI composite.....	32
Figure 20. Fracture surface appearance of IM7/BMI composite with 9301 finish .....	33
Figure 21. Fracture surface appearance of IM7/BMI composite with 9301 finish .....	34
Figure 22. Fracture surface appearance of IM7/BMI composite with 9301 finish .....	35
Figure 23. Fracture surface appearance of IM7/BMI composite with 9301 finish .....	36
Figure 24. Galvanic corrosion samples after 2 days of immersion .....	37
Figure 25. Weight changes after 2 weeks of immersion.....	38



## FIGURES (concluded)

Figure 26. Surface appearance of unsized IM7/BMI control corrosion specimens.....	39
Figure 27. Corrosion surface appearance with PH9301F finish at 500X.....	39
Figure 28. Corrosion surface appearance with PH9304F finish.....	40
Figure 29. Corrosion surface appearance with PH9305F finish.....	40
Figure 30. Corrosion surface appearance with PH9306F finish.....	40
Figure 31. Corrosion surface appearance of unsized composite below water line .....	41
Figure 32. Corrosion surface appearance of PH9304F finished composite below water line .....	41
Figure 33. Appearance of aluminum anode coupled to unsized control composite .....	42
Figure 34. Appearance of aluminum anode coupled to PH9301F finished composite .....	42
Figure 35. Appearance of aluminum anode coupled to PH9304F finished composite .....	43
Figure 36. Appearance of aluminum anode coupled to PH9305F finished composite .....	43
Figure 37. Appearance of aluminum anode coupled to PH9306F finished composite .....	43
Figure 38. Room temperature longitudinal flexural strengths for IM7/BMI composites.....	45
Figure 39. Room temperature short beam shear strengths for IM7/BMI composites.....	45
Figure 40. Sample capacitance versus exposure time for control and coupling agent modified composite samples tested to expose fiber lengths .....	48
Figure 41. Sample capacitance versus exposure time for control and coupling agent modified composite samples tested to expose fiber ends.....	49





## TABLES

Table I.	DSC Characterization Results at 10°C/min for Reactive Coupling Agents .....	18
Table II.	Solubility of Reactive Coupling Agents in Protic Solvents .....	19
Table III.	Solubility of Reactive Coupling Agents in Aprotic Solvents.....	19
Table IV.	DSC Characterization Results at 10°C/min for Reactive Finishes .....	23
Table V.	Finish Coating Thickness.....	24
Table VI.	Voltage Contrast XPS Results on BMI Matrix Rods.....	30
Table VII.	Calculated Debonded Area from EIS Measurements .....	44
Table VIII.	Mechanical Properties of BMI Matrix Composites .....	46
Table IX.	Calculated Debonded Area for Longitudinal EIS Measurements.....	49
Table X.	Calculated Debonded Area for End-On EIS Measurements .....	50



## EXECUTIVE SUMMARY

The objective of this program is the development and demonstration of galvanic corrosion resistant carbon/BMI composites through the use of reactive finishes to form coatings that isolate the carbon fibers from the BMI matrix. A family of novel reactive coupling agents was formulated into phenolic-based finishes for carbon and graphite fibers that will subsequently react with the fiber and matrix resin during processing to form chemical bonds at the interface and in the interphase. In this process, each fiber is coated uniformly with the phenolic finish and bonded to the finish before the BMI prepregging process. The finish serves to isolate the carbon fibers from the BMI matrix and interrupts the galvanic cell.

Results show that this approach is a viable means of improving galvanic corrosion resistance of carbon/BMI composites and that composite mechanical properties are not compromised by the finish. Both static measurements on galvanic corrosion couples and dynamic electrochemical impedance spectroscopy measurements show that all but one of the four finishes examined dramatically improve composite corrosion resistance. Flexural and short beam shear measurements show that BMI matrix composites with finished fibers are equivalent to those with unsized fibers. The mechanical data is supported by VCXPS measurements and SEM failure surface analysis that show that interfacial adhesion is superior in the finished composites. When optimized, this approach has the potential to dramatically improve galvanic corrosion resistance of the interface in BMI matrix composites by preventing the interfacial debonding thought to be responsible for the observed reaction acceleration.

The addition of reactive finishes to fiber surfaces serves the dual purposes of protection of the fiber during handling and alteration of the interphase in the cured composite. The surface protection aspect of finishes will become even more critical as composites technology focuses on the use of 3-D braids and weaves for development of low cost composite processes, such as transfer molding. The reactive finish approach will provide a cost efficient means of improving galvanic corrosion resistance in composites with any BMI formulation.



## INTRODUCTION

Carbon/bismaleimide (BMI) composites are the best material candidates for a number of aerospace applications that require thermal stabilities in the 250°F to 350°F temperature range. There has been considerable effort expended in the synthesis, formulation, development, and qualification of BMI composites over the last fifteen years. The technology has developed to the point that state-of-the-art BMI resins even have toughnesses comparable to those of lower temperature epoxy systems. One problem that has limited the use of BMI composites is the system susceptibility to galvanic degradation.

Carbon-reinforced imide composites degrade when they are electrically connected to certain metals in the presence of salt water. Most workers agree that the mechanism responsible for the observed effect involves hydroxyl attack on the imide ring [1-4]. Other possibilities include direct reduction of the imide ring [5,6], reactions related to the Hoffman Degradation [7] mechanism used in production of amines from amides, and polarization effects at the fiber surface [8]. Although the specifics of the mechanism are not fully known, it is clear that a requirement for the observed degradation to occur is that the BMI composite be the cathode in a galvanic cell. Any interruption of the cell circuit will prevent the BMI degradation and also the associated galvanic metal corrosion.

In structural applications, the galvanic couple is produced by the mechanical fastening of composite to metal. Recognition of galvanic effects in carbon/epoxy-aluminum couples in the 1970s led to the development of isolation schemes that were designed to interrupt the circuit. The barrier system typically includes a fiberglass composite ply cured into the surface of the carbon ply, primer coat applied to the metal in the joint area, and curing sealant (polysulfide) wet-applied to the fastener that is used to connect the metal and composite.

There is some disagreement on the effectiveness (or even the need) for galvanic protection in BMI - aluminum couples. Work performed at General Dynamics and BASF Corp. [9] indicated that composite bearing strength of galvanically coupled materials was not affected by a 2000 hr. exposure to salt spray even when no surface coatings were applied to either member of the couple. However, a series of systematic studies performed at the Naval Air Warfare Center (NAWC) [2,10,11] demonstrated that the type of protection scheme used in carbon/BMI-aluminum couples was critical and further that the degree of protection, as defined by visual inspection after exposure and by bearing strength measurements, was directly related to the coating quality of the specific systems used. When the coating remained tightly bonded to the surface of the composite, the amount of degradation observed in the experiment was significantly reduced relative to uncoated or "poorly" coated samples. Another interesting finding in the NADC work was that the presence of sealant in the hole around the fastener did not improve resistance to



the degradation process as anticipated but rather, resulted in a greater reduction in composite strength compared to unsealed samples. The proposed explanation was that the sealant allowed the electrolyte to be concentrated in the hole.

The effects observed in the isolation scheme study can be attributed to difficulties associated with adhesion of coatings to the BMI composites. It has been found that conventional, epoxy composite-compatible paints and coatings do not adhere well to BMI composites especially after environmental conditioning. Also, it should be noted that the carbon exposed by cutting through a composite will be extremely inert and that this carbon/BMI composite surface will be resistant to secondary bond formation.

A more dependable long term solution would be to apply a well bonded, nonimide uniform coating around each fiber in the composite. This approach functions by electrical isolation of the carbon fibers and interruption of the galvanic cell. All of the proposed degradation mechanisms should be prevented by such an action. From a reliability standpoint, the development of an improved fiber finish system that could be applied to carbon fibers and used with BMI resin systems already in existence would be the best solution to the galvanic degradation problem. In this work, we distinguish a finish as an adhesion-promoting chemistry applied to a fiber surface from a sizing, which is applied as a handling aid.

The quality of the interface has often been cited as a critical parameter that controls the performance of all composites. The interface region in carbon fiber-reinforced composites is a complicated, multilayer zone consisting of the carbon near surface, carbon-finish or matrix interface, and finish-matrix interface or matrix interphase. Each of these zones must be understood and controlled to produce a well-adhered system capable of delivering the required composite mechanical performance while also affording galvanic protection in imide-based composites.

Work has been performed on the characterization and modification of the interphase material that is present between the fiber and bulk matrix resin in the composite. This interphase can form naturally either as a result of altered chemical reaction kinetics in the region adjacent to the fiber surface [14], or as a result of the interaction between the sizing applied to the fiber prior to processing and the resin [13-15]. In some cases, coatings that are designed to afford specific characteristics to the composite system, such as stiffness or toughness, have been purposely applied to the fiber [16-19].

It has been found that each of these approaches can improve composite properties. The extension of the interphase modification concept through the use of reactive finishes for improvement of the galvanic corrosion resistance of imide-based, high temperature composites offers the potential to dramatically enhance the performance of the systems that are currently available. The reactive finish



concept is shown schematically in Figure 1 where the finish chemically bonds to the fiber surface and to the polymer matrix to provide a well bonded, durable interphase to isolate the BMI matrix from the carbon fiber.

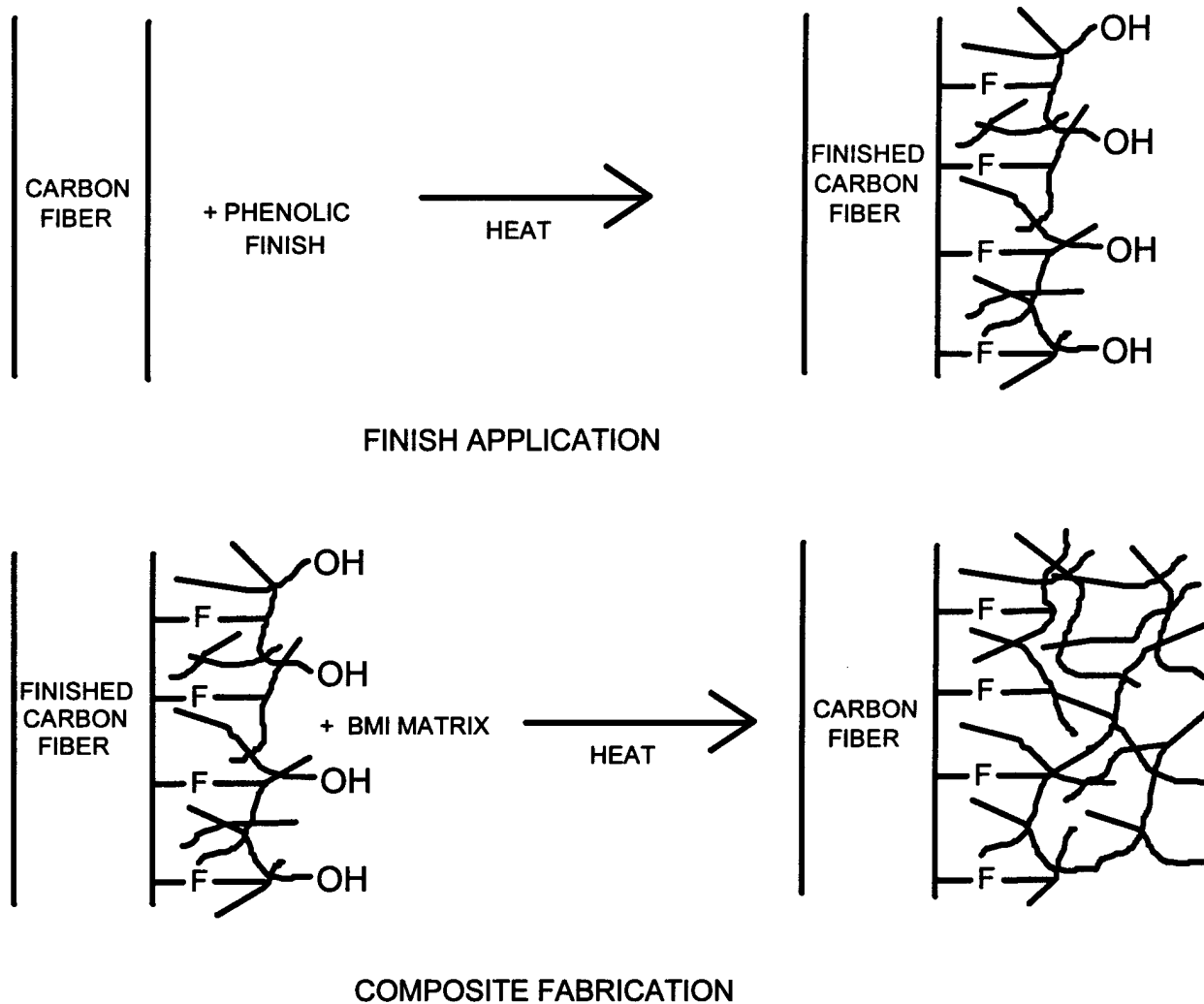


Figure 1. Reactive finish interfacial bonding concept

The overall objective of this program was to develop a well-bonded nonimide finish or coating for carbon fibers to reduce galvanic corrosion of imide-matrix composites. The approach taken was to formulate a finish consisting of a phenolic resin, a coupling agent that is reactive with both the carbon fiber and phenolic resin, surfactants, and solvents. Mixtures of some of these ingredients are often necessary for solubility and processing reasons. The finish is applied to carbon fiber tows using a dip process followed by thermal activation of the coupling agent. The finish must be uniform and thick enough to serve as a corrosion barrier while not compromising overall composite performance.



Results show that the approach taken provides well-bonded phenolic coatings to the individual carbon fibers in a 12K tow that subsequently provide a well-bonded interface to a BMI matrix in the composite. Galvanic corrosion tests verify that the finished composites have significantly greater corrosion resistance than control composites fabricated with unsized carbon fibers.

## EXPERIMENTAL PROCEDURES

### Materials

12K IM7 unsized carbon fibers were obtained from Hercules, Inc. (Magna, UT). Phenolic (Georgia Pacific 5236) and BMI (Ciba-Geigy Matrimid 5292) resins were purchased from Applied Poleramic, Inc. (Benecia, CA). All other chemicals were used as-received from Aldrich Chemical Co. (Milwaukee, WI).

### Coupling Agent Synthesis and Characterization

The first step in the program was to synthesize additional quantities of reactive coupling agents using previously developed techniques. Figure 2 depicts the generic structure of the proprietary coupling agents. The synthesis was carried out with controlled laboratory conditions for four variations of the structure shown in Figure 2.

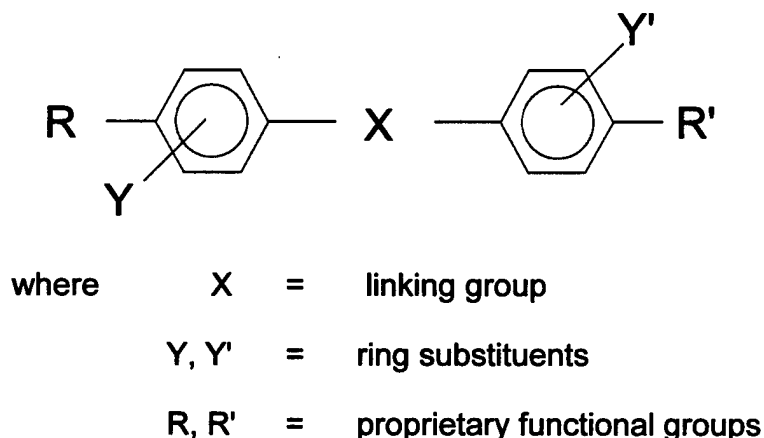


Figure 2. Schematic chemical structure of reactive coupling agents

Verification of product purity was performed using a Mattson Cygnus 100 FTIR spectrophotometer. FTIR spectra were obtained on a sample of known purity and compared to the synthesized material. Thermal properties of the coupling agents were determined using a Perkin Elmer Series 7 differential scanning calorimeter (DSC). The synthesized coupling agents were shown to be in excess of 97% purity and were used as-produced for preparing the finish formulations. Solubility of the coupling agents in protic and aprotic solvents was determined by dissolving the



coupling agents in the stirred solvent at 23 and 55°C for 1 hour and filtering the undissolved compound.

### Finish Formulation Development

Initial finish formulations using four variations of the generic coupling agent shown in Figure 2 contained 10 wt.% phenolic and 0.1 wt.% coupling agent in acetone. A high polymer content was attempted to try to protect the reactive intermediates from oxidation during processing and to provide a thick barrier coating on the fibers. Ten percent phenolic proved to be too much and resulted in stiff impregnated bundles of fiber that would be difficult to fabricate into composites. Reduction of the phenolic in those solutions to 1.0% produced better handling finished fibers.

Bonding of the finish to the carbon fibers before prepregging is felt to be necessary so that the finish cannot be removed in the solvent of a prepreg impregnation bath or diffuse into the imide matrix during a hot melt prepreg process. Partial curing of the phenolic also improves the handling characteristics of the finished fiber tows for use in subsequent processes such as weaving, braiding, or filament winding.

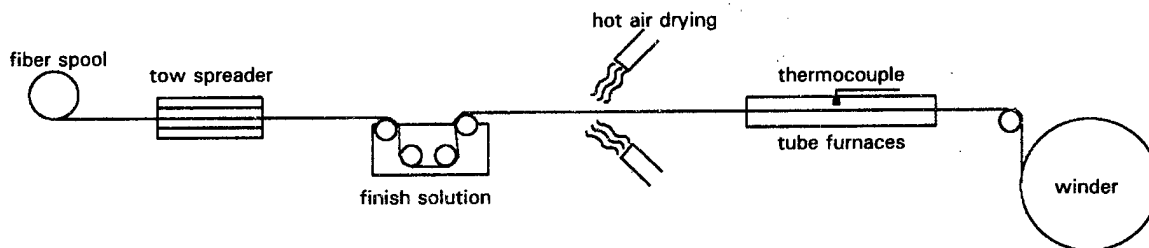
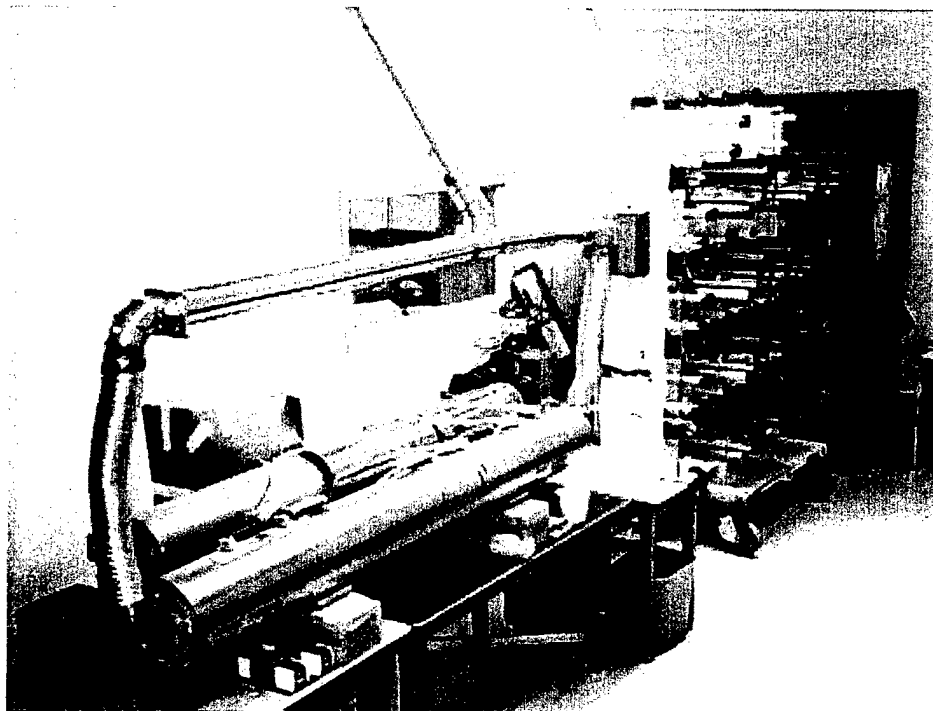


Figure 3. Schematic of finish application apparatus

A photograph of the finish processing line is given in Figure 4.

The set-up shown in Figures 3 and 4 is designed to spread the fiber tow allowing even coating of each fiber with the finish solution and drying before recollimating the tow so that fibers do not stick together. The drying step is accomplished with hot air blown over the fibers, which eliminates solvent and reduces the chance of the fibers sticking together in the tube furnaces. After the finishing process, the fiber tows were supple and appeared compatible with subsequent prepregging processes.



*Figure 4. Finish processing line*

Numerous formulations were prepared with the four reactive coupling agents. Formulation variables included concentrations of coupling agent and phenolic. Finish cure temperature was also evaluated in the set-up shown in Figures 3 and 4. Finished fiber samples thought to be of good quality from appearance and feel (*i.e.*, not too stiff and without fibers stuck together) were selected for further evaluation.

The selected finished fiber sample lots were then divided in half. One-half was saved for scanning electron microscopy (SEM) evaluation in the as-finished condition. The other half of each lot was soaked in acetone at room temperature for 2 hours. The acetone soak was conducted to evaluate the fiber-finish bonding. Unbonded finish should be removed by the acetone wash. Acetone soaked samples were then evaluated using SEM.

An additional screening test was used to aid in the selection of the finish formulations to use in the composite corrosion studies. The coupling agent-to-phenolic carrier ratio in the finish determines the mechanical properties (strength, stiffness, toughness) of the interphase region. Desired properties of the interphase region are unknown and beyond the scope of this program. Preparation of an interphase with moderate thickness, stiffness and toughness was attempted in this program. An initial feel for the finish mechanical properties was obtained by bending the fibers over a small radius and observing for evidence of cracking.





Single fibers were spirally wound around a small-diameter cylindrical core to investigate the integrity of the fiber coatings when subjected to small bending radii. Approximately 3-7 single fibers (filaments) were removed from a yarn and spirally wound around a 0.046-inch (1.18 mm) cylindrical core. The core was mounted to an aluminum stem with silver conductive paint. The specimens were sputter-coated with gold (Au) for 30 seconds at 50 mTorr and 40 mA using a Denton Vacuum DESK II Cold Sputter/Etch Unit to a thickness of approximately 100 angstroms. The fiber surfaces were analyzed and the mean fiber diameters were measured using an AMRAY 1830 scanning electron microscope at 20 keV.

### **Finish Characterization**

Thermal properties of the finish formulations were determined using a Perkin Elmer series 7 differential scanning calorimeter (DSC) and evaporating small droplets ( $\approx 20$  mg) of the finish in the DSC pan. DSC measurements were made at a heating rate of  $10^{\circ}\text{C}/\text{min}$ .

### **Prepreg Fabrication**

Prepregs were manufactured by drum winding the fiber dry followed by resin impregnation using a known amount of BMI resin solids. Dry IM7 fibers were first wound at a rate of 6.7 turns per cm to a width of 22.5 cm, which when cut yielded prepregs with dimensions of 22.5 x 60 cm. BMI resin dissolved in methylene chloride to 43% solids was applied at a rate of 225 g per winding. The resin was applied from solution using a brush. Prepregs were allowed to dry in air and then removed from the drum and an additional 180 g of BMI solution applied to the back side of the prepreg. After drying, the prepreg was very stiff and boardy. Prepreg weights were recorded to determine weight percent resin. Variations in fiber and resin content in the prepregs were within  $\pm 2\%$  from one prepreg to the next, demonstrating good reproducibility in prepreg manufacturing. Prepregs were then wrapped in polyethylene and aluminum foil and stored at  $-18^{\circ}\text{C}$  until needed for the composite panel fabrication. Five types of prepreg were fabricated for this study. A control fiber using Hercules IM7 12K and that same fiber finished with PH9301F, PH9304F, PH9305F, and PH9306F were produced.

### **Composite Processing**

The first composites produced in the program were 12K tow rods with a BMI matrix. The rods were produced in a modified version of the finishing line shown in Figures 3 and 4. A resin impregnation bath was added in place of the finish solution bath followed by a wire drawing die to form the impregnated tow into a rod and remove excess BMI resin. The BMI resin bath contained 60% solids in methylene chloride. After being pulled through the wire drawing die, the impregnated rod was drawn into the tube furnaces and held at  $200^{\circ}\text{C}$  for 30



minutes. The cured rods were then removed from the furnaces and cut into 30 cm lengths before being postcured in air for 1 hour at 180°C followed by 2 hours at 200°C and, finally, 6 hours at 250°C. The resultant rods were very smooth with no visible voids on their surfaces. Polished cross sections also showed no visible voids when viewed with an optical microscope.

Unidirectional composites were fabricated using a vacuum bag hot press molding technique in hard tooling. Eight ply stacks of staged prepregs were used to fabricate the unidirectional composites for the corrosion studies. The cure cycle is shown in Figure 5.

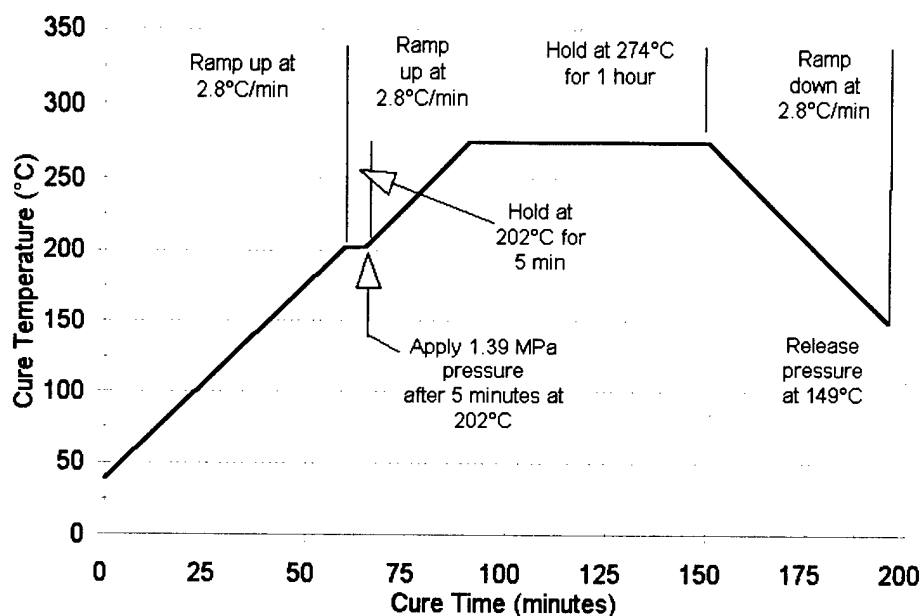


Figure 5. Composite cure cycle for BMI matrix panels

The molded composite panels had a final 0.20 cm (0.080 in.) thickness.

### Composite Panel Characterization

Laminate quality was confirmed with metallographic analysis on polished cross sections, ultrasonic C-scan inspection, optical microscopy, and thermal analysis. Only materials with less than 2% voids and representative glass transition temperatures ( $T_g$ s) were selected for mechanical testing. Ultrasonic nondestructive inspection was performed on the composite panels using an Ultra Image IV system. Standard procedures developed for BMI matrix composite systems were used for interpretation of the scans.

$T_g$ s were determined with a Rheometrics RMS 800 using a torsion/rectangular configuration at a heating rate of 5°C per minute.



## Mechanical Testing

Flexure testing on 0°, 90°, and short-beam shear specimens at room temperature and at 177°C was conducted in accordance with ASTM D-790 and ASTM D-2344 on a 22 Kip capacity MTS Model 810 servohydraulic test frame and an upgraded 22 Kip Instron Model TTD-L screw-driven test frame. A 10:1 span to depth ratio was used for both flexure tests and a 4:1 ratio was used for the SBS tests. Testing was performed at a rate of 0.02 cm/min.

Compression tests were conducted in accordance with ASTM D695. The initial loading rate was 0.02 cm/min to a strain of 16 percent followed by a rate of 0.1 cm/min until specimen failure.

All elevated temperature testing was performed using an Instron Model 3111 temperature chamber at 177°C. Thermocouples were placed in contact with the test specimens in the chamber and monitored. Specimens were allowed to equilibrate for 2 minutes before the tests were run.

Moisture saturation was performed at 94°C in distilled water for a period of 42 days. The average weight gain due to moisture absorption for the control and PH9304F finished specimens was 2.4 and 1.6 percent, respectively.

## Spectroscopic Characterization

Additional characterization was conducted on the 12K rod test specimens using voltage contrast X-ray photoelectron spectroscopy (VC-XPS) after the technique given in Refs. 20-22. The specimens were split to expose a fresh transverse surface and the ratio of carbon in the fiber ( $C_f$ ) to carbon in the matrix ( $C_m$ ) measured on a Fisons Escalab MKII instrument with 20 eV Mg  $\alpha$  X-rays and electrons on a 5 x 2 mm spot size. The electrons selectively charge the nonconductive resin matrix portion of the surface and separate their emitted photoelectron signal from that of the conductive fibers.



## Galvanic Corrosion Testing

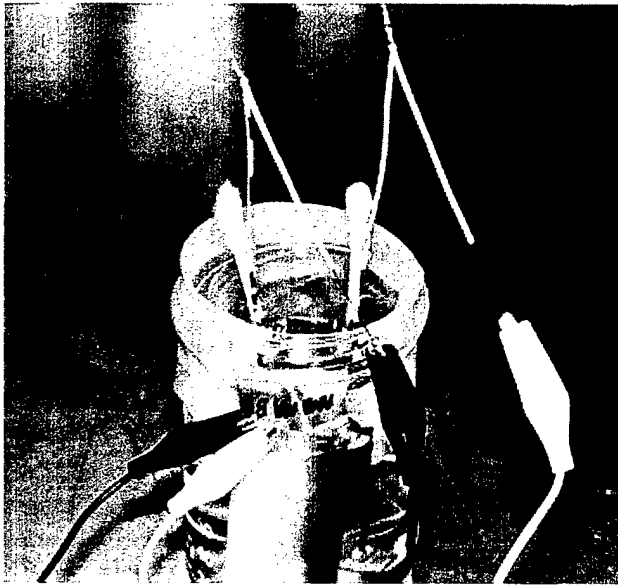
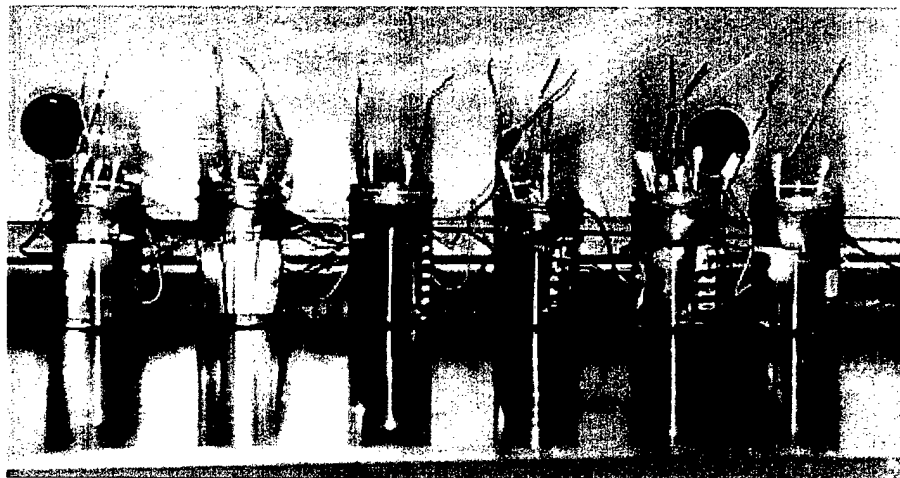


*Figure 6. Galvanic corrosion sample setup*

used to further support the rods where they penetrated the plastic cup lid. The entire matrix of corrosion samples (4 finished, 2 controls) is shown in Figure 7.

The first electrochemical study involved galvanic couple corrosion experiments with BMI matrix composite rods (1 12K tow) joined to aluminum in salt water. Rods of each type (unsized or one of 4 finishes) were coupled to a large "L"-shaped piece of 5052-H39 aluminum foil with a corrosion-resistant coating and connected with jumper wire. The assembly was then immersed in 3.5 wt.% salt water approximately half-way up the rods to form the corrosion sample. A photograph of a typical sample is shown in Figure 6. The bottom of a plastic cup held in place with parafilm was used to support the composite rods. Cotton swabs were

*Figure 7. Complete set of galvanic corrosion samples*



The coupled samples were monitored for signs of corrosion daily. Current and voltage readings were taken at regular intervals, but proved to be unrevealing.

## Electrochemical Impedance Spectroscopy

Electrochemical impedance spectroscopy (EIS) on BMI-matrix composites was first run on duplicate sample rods fabricated for the static corrosion experiments. The cut ends of the composite rods were sealed with Microstop electroplater's lacquer to



allow only the sides of the rods contact with the solution. Tests were run in 3.5% salt water with a standard three electrode cell (nichrome mesh counter electrode, calomel reference electrode, and the sample). A 10 mV signal was then applied over the frequency range between 10 kHz and 100 mHz and the phase shift monitored to get the baseline data. A capacitance was then calculated that corresponds to the exposed carbon area in the composite.

Cathodic disbondment was then artificially induced by potentiostatically polarizing samples at  $-1.4 V_{scc}$ . The degree of disbondment was periodically measured using electrochemical impedance spectroscopy (EIS). EIS was conducted by applying a 10 mV sinusoidal voltage wave at frequencies ranging from 65 kHz to 100 mHz at a sampling rate of 10 points per decade. This test was repeated several times over the exposure period.

Following the initial study on 12K rods, fiber reinforced composite samples modified with different finish compositions were tested for susceptibility to cathodic disbondment during cathodic polarization in aerated 3.5% NaCl solution. Cathodic disbondment occurs due to degradation of the polymer matrix phase that occurs when local alkalinity develops at exposed carbon fibers during the test. Two test configurations were examined in this survey. In the first configuration, composite samples were potted in epoxy end-on and polished through to a 600 grit finish using SiC papers. In this arrangement, fiber ends were exposed for testing without exposing fiber lengths. In the second configuration, surfaces of composite panels were exposed to the test solution directly. In this arrangement, fiber lengths were exposed without exposing fiber ends. Electrical connection was made to all of the fibers by abrading the opposite end of the samples and affixing a Ni-Cr wire using silver epoxy.

## RESULTS AND DISCUSSION

### Coupling Agent Characterization

A sample DSC thermogram for the AT-CA-9306 coupling agent is shown in Figure 8. The thermogram in Figure 8 shows the sharp endothermic melting of the crystalline coupling agent at 44°C followed by a wide ranging decomposition exotherm beginning at 131°C continuing to 200°C.

Similar features are seen in the DSC thermograms for all the coupling agents. A summary of the coupling agent DSC results is given in Table I. The DSC data describes the melting point ( $T_m$ ) and decomposition temperature ( $T_d$ ) range for the bonding reaction for each reactive coupling agent.

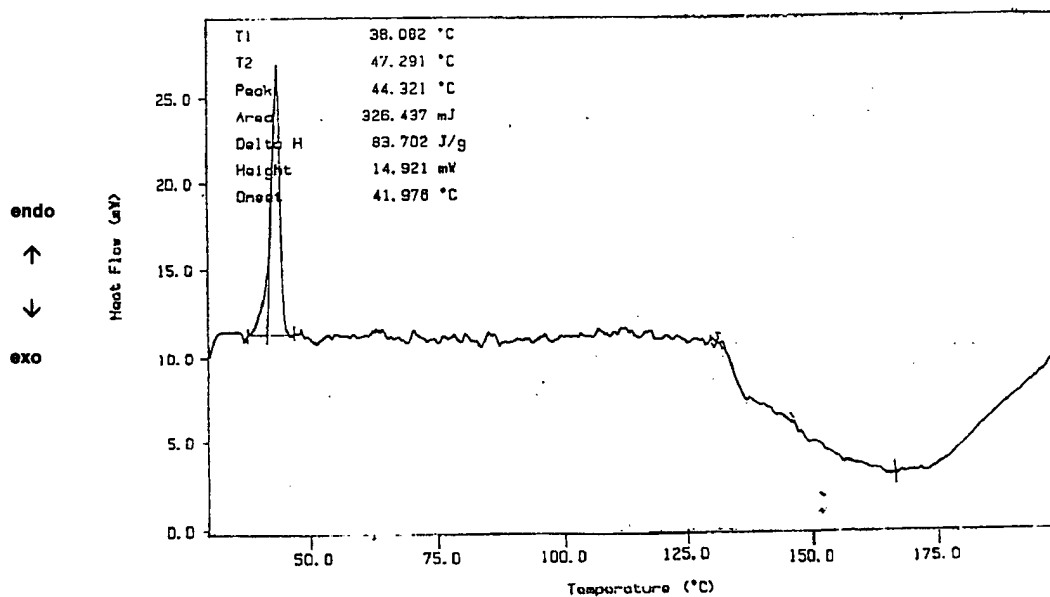


Figure 8. DSC thermogram at 10°C/min for AT-CA-9306 reactive coupling agent

Table I. DSC Characterization Results at 10°C/min for Reactive Coupling Agents

Coupling Agent	T <sub>m</sub> (°C)	ΔH <sub>melt</sub> (J/g)	T <sub>d</sub> onset (°C)	T <sub>d</sub> max (°C)	T <sub>d</sub> end (°C)	ΔH <sub>d</sub> (J/g)
AT-CA-9301	*	--	135	170	**	- 881
AT-CA-9304	137	52.8	138	144	163	-528
AT-CA-9305	*	--	116	165	195	-449
AT-CA-9306	44	83.7	131	165	200	-859

\*Not evident.  
 \*\*Peak 2 onset 185, max 196, end 215.

Solubility of these coupling agents was also determined in protic and aprotic solvents. Solubility results are given in Tables II and III.

The solubility results given in Tables II and III show that every coupling agent is soluble to some degree in one or more of the solvents tried. Based upon the results given in Table III and the solubility parameter of phenolics, acetone was chosen as the initial solvent for the finish formulations.



**Table II. Solubility of Reactive Coupling Agents in Protic Solvents**

Coupling Agent	Protic Solvents at 23°C/55°C				
	Water	Methanol	Ethanol	1-Propanol	2-Propanol
AT-CA-9301	N/N	SL/SL	VS/VS	VS/VS	VS/VS
AT-CA-9305	N/N	VS/VS	N/N	VS/VS	VS/VS
AT-CA-9306	N/N	SL/SL	VS/VS	VS/VS	VS/VS
N Not soluble.		SL Slightly soluble.			
VS Very slightly soluble.		S Completely soluble.			

**Table III. Solubility of Reactive Coupling Agents in Aprotic Solvents**

Coupling Agent	Aprotic Solvents 23°C/55°C					
	Acetone	Methyl-Ethyl Ketone	Methyl-Isobutyl Ketone	Toluene	Methylene Chloride	Chloroform
AT-CA-9301	S/S	S/S	S/S	VS/VS	SL/S	SL/SL
AT-CA-9305	SL/S	SL/S	SL/SL	SL/SL	S	S
AT-CA-9306	S/S	S/S	S/S	VS/VS	SL/S	SL/SL
S Completely soluble.		VS Very slightly soluble.		SL Slightly soluble.		

The coupling agents display a range of melting points, reaction onset temperatures, maximum reaction temperatures, and solubilities. That variability allows finishes to be tailored to the desired processing and cure cycle for the composite.

**Finish Characterization**

DSC thermal characterization of the standard finish compositions containing the reactive coupling agents was conducted. The phenolic diluent in the finishes was also run neat. DSC thermograms for each system are shown in Figures 9-13. The phenolic resin (Figure 9) shows a series of melting endotherms between 75 and 90°C, a large endotherm near 100°C, and a curing exotherm at higher temperatures. The low-temperature endotherms in the phenolic (Figure 9) are due to melting of the base catalysts, paraformaldehyde and hexamethylenetetraamine, their decomposition products, and, perhaps, some crystallites in the phenol from hydroquinone [23]. The large endotherm near 100°C is due to water elimination.

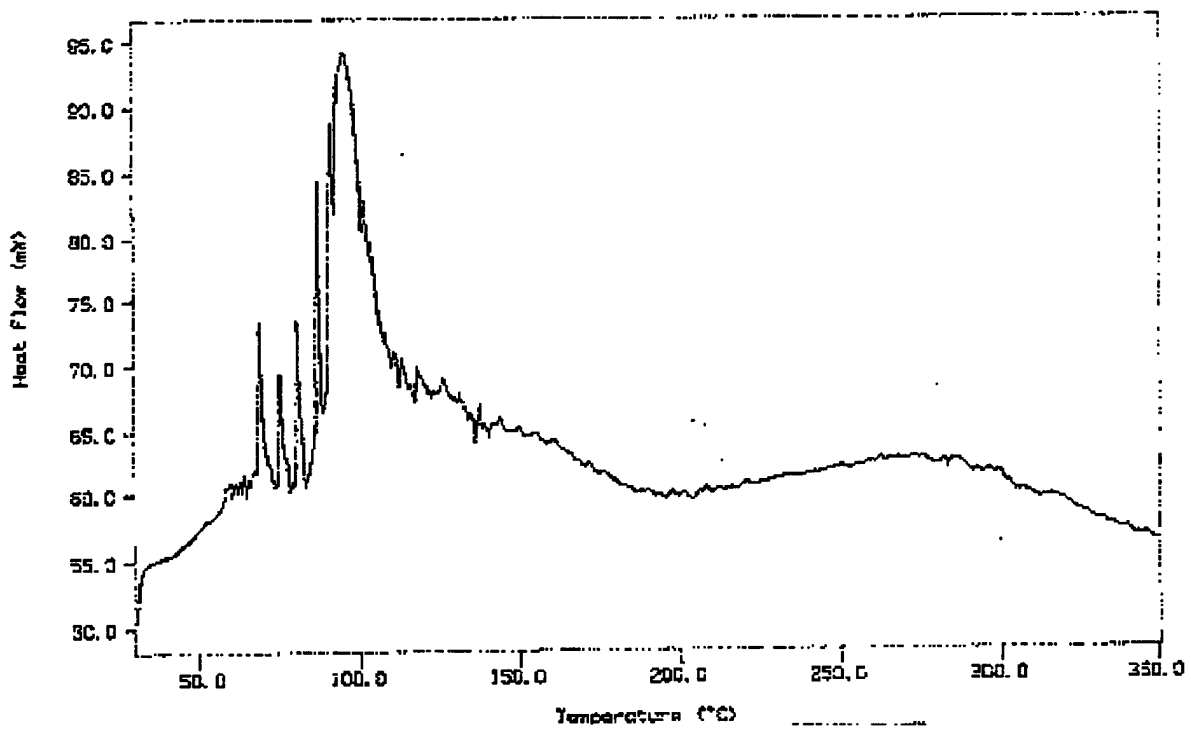


Figure 9. DSC thermogram at 10°C/min for neat phenolic resin

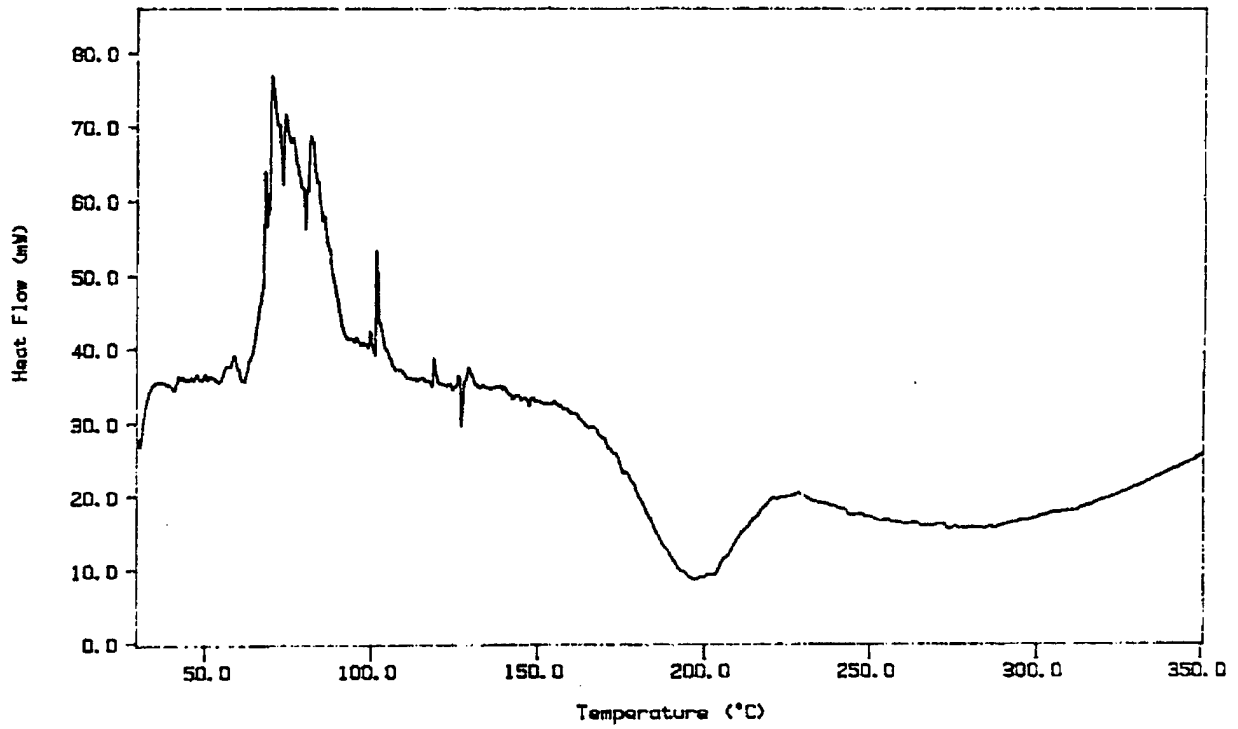


Figure 10. DSC thermogram at 10°C/min for PH9301F finish





The PH9301F system does not show the sharp melting endotherms present in the neat phenolic between 75 and 90°C. Apparently, the crystallites dissolved in the acetone and did not reform upon drying. The PH9301F thermogram does show the large water elimination endotherm followed by a strong exotherm beginning at 160°C with a maximum at 195°C ending at 220°C. That exotherm is followed by another small exothermic region up to 280°C where the reaction again becomes endothermic. Note that the coupling agent reaction exotherm has shifted to higher temperatures in the finish than in the neat condition. The reason for the shift is unknown. It may be that the local chemical environment in the neat material is more electron rich than in the presence of the polymer diluent, which would weaken the active bonds causing reaction at a lower temperature or energy. The high-temperature endothermic behavior may be an artifact from baseline drift in the instrument above 300°C.

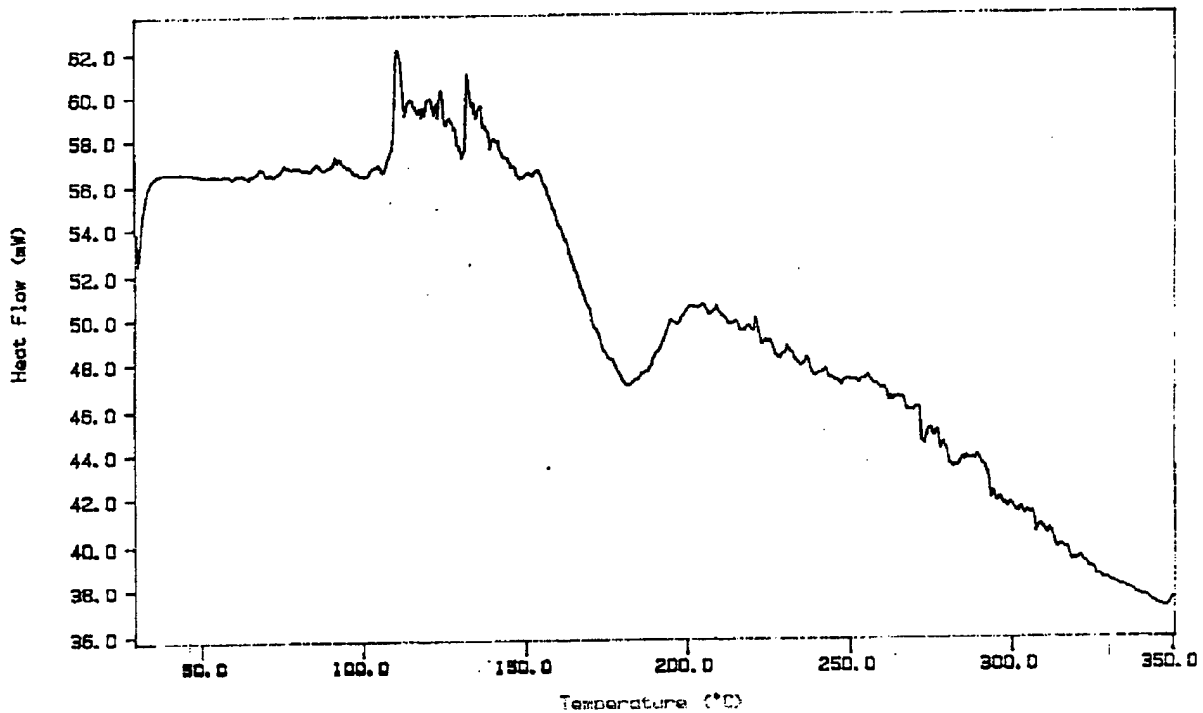


Figure 11. DSC thermogram at 10°C/min for PH9304F finish

The PH9304F finish thermogram given in Figure 11 shows similar thermal activity to the PH9301F, again exhibiting a shift in the reaction exotherm to higher temperatures. Following the reaction exotherm, the PH9301F finish has a high-temperature exotherm that is expected from the phenolic contribution to the thermogram.

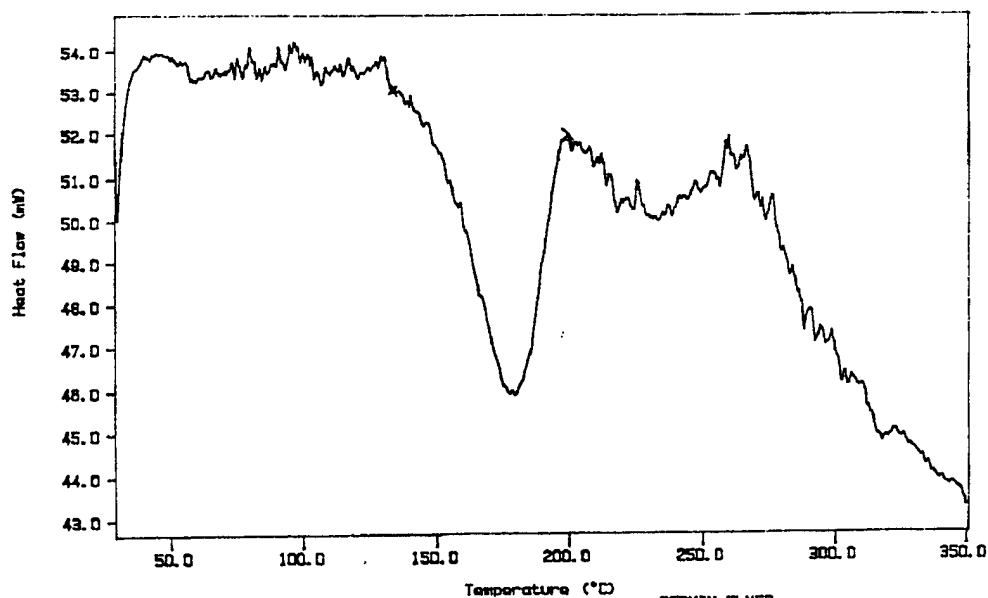


Figure 12. DSC thermogram at 10°C/min for PH9305F finish

The PH9305F and PH9306F finishes display similar behavior to that of the PH9304F. The PH9305F and PH9306F finishes (Figures 12 and 13) show only small endothermic peaks corresponding to water elimination. Free water in the phenolic comprises the major amount of water evolved. Apparently, those two samples were dried to a greater extent than the PH9301F and the PH9304F before the DSC runs. The coupling agent decomposition exotherm is again shifted to higher temperatures in the PH9305F and PH9306F finishes compared to the neat compound.

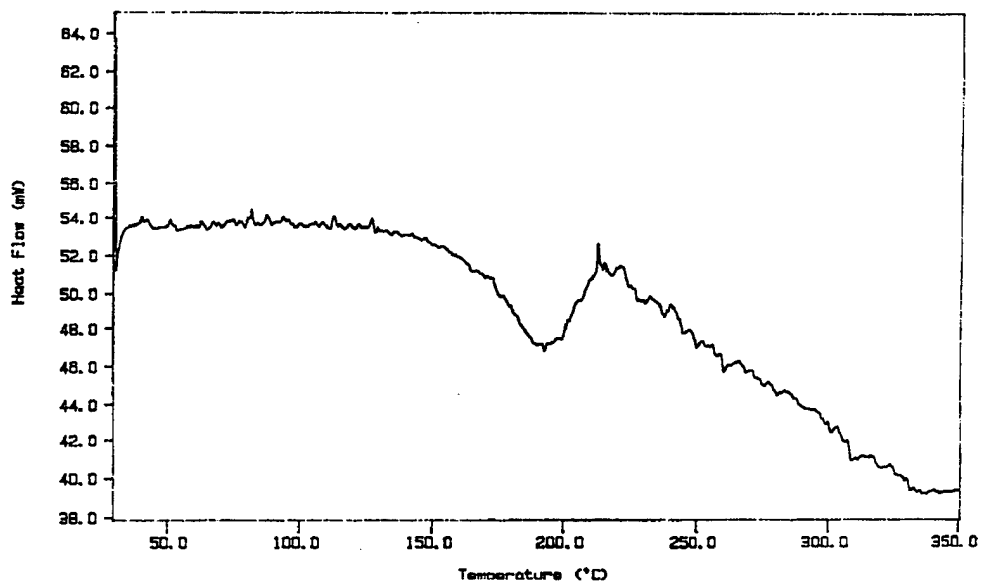


Figure 13. DSC thermogram at 10°C/min for PH9306F finish



A summary of the finish DSC data is given in Table IV.

**Table IV. DSC Characterization Results at 10°C/min for Reactive Finishes**

Finish	T <sub>m</sub> (°C)	ΔH <sub>melt</sub> <sup>1</sup> (J/g)	T <sub>d</sub> onset (°C)	T <sub>d</sub> max (°C)	T <sub>d</sub> end (°C)	ΔH <sub>d</sub> (J/g)
Phenolic, neat	69-95 <sup>2</sup>	262	155	195	272	-178
PH9301F	70-90 <sup>2</sup>	147	173	196	227	-136
PH9304F	111-132 <sup>2</sup>	53	154	183	202	-95
PH9305F	80-131 <sup>2</sup>	5	156	178	200	-149
PH9306F	3	--	173	193	213	-120

1. Includes water evolution.  
2. Series of peaks.  
3. Not evident.

Taken together, these results show that the coupling agent reaction is complete before initiation of the phenolic curing reaction. This allows the bonding reaction to be controlled independently from the polymer cure, which gives increased control to the overall process.

Examination of the finish thermograms reveals the following observations:

- ❖ Melting points seen for the coupling agents are not evident in the finish mixtures. This shows that the coupling agents are molecularly dispersed in the mixtures and do not exist as islands of crystalline material, which would be detrimental to performance.
- ❖ The crystalline melting endotherms from the phenolic ingredients are likewise not evident in the finishes for the same reason.
- ❖ The modified electronic environment of the coupling agents in the finishes causes a shift in their decomposition temperature to higher temperatures.

Attempts to fabricate bulk castings of the finish compositions for thermophysical measurements were unsuccessful. Several difficulties were encountered that may prevent castings from being prepared by any means. The coupling agents are insoluble in the phenolic at room temperature in high concentrations. Once the



solvents used to compound the finish components begin to flash off in preparation for curing the final mixture, the coupling agent phase separates. That is unacceptable because the resulting network would not look like that of the finish thin film on the fibers even if a final cure were possible. This effect occurred with numerous solvent types and mixtures of solvents. As such, the solvent approach was abandoned. Additional attempts to fabricate bulk castings of the finish compositions for thermophysical measurements from the melt resulted in the formation of organic foams of little value. The thermophysical properties of the cured finishes will have to be implied from the composite aging behavior.

### Finish Development

Thermal activation of the finish was successful with the set-up shown in Figures 3 and 4 at a temperature of 200°C. Numerous coating trials were conducted for applying the reactive finish to determine the effects of finish formulation and processing parameters on the final finish uniformity, thickness, and subsequent reactivity with the carbon fiber surface. Results of the finishing trials are given in Table V.

**Table V. Finish Coating Thickness**

Finish System	Initial Diameter (Microns)	Diameter After Acetone Wash (Microns)	Change (%)
None	5.0*	--	--
PH9301F**	7.1 ± 0.2	7.0 ± 0.1	-1.4
PH9304F	6.7 ± 0.2	6.9 ± 0.1	+3.0
PH9305F (lot 1)	6.6 ± 0.1	6.5 ± 0.1	-1.5
PH9305F (lot 2)	6.1 ± 0.3	6.5 ± 0.1	+6.6
PH9306F	7.0 ± 0.1	7.0 ± 0.1	0
* Hercules' Product Data Sheet 868 for IM7 Carbon Fiber. ** 0.01% coupling agent and 1.0% phenolic in acetone.			

The thickness data given in Table V show that the finish coating thickness varies between 0.75 and 1.0 μ, which is in the expected desired range for galvanic protection of the imide matrix material.



The finished fibers were then characterized by SEM for uniformity and thickness of finish and bonding to the carbon fibers. Bonding was examined by soaking the finished fibers in acetone for 2 hours before the SEM analysis. The surface appearance of unsized IM7 fibers is smooth and featureless as shown in Figure 14. Figures 15-18 show SEM photomicrographs of finished fibers before and after acetone wash for each of the four finishes. The finish coating is readily apparent and generally uniform on the fibers. This shows that the phenolic is a good film former for use as the finish base. For the most part, little of the finish is removed by an acetone wash, which shows that the processing conditions studied are adequate to initiate the coupling reaction and that the desired bonding is taking place. Some excess coating is also apparent as are areas where the fibers have stuck together; however, after finishing the tow has excellent handle for subsequent processing.

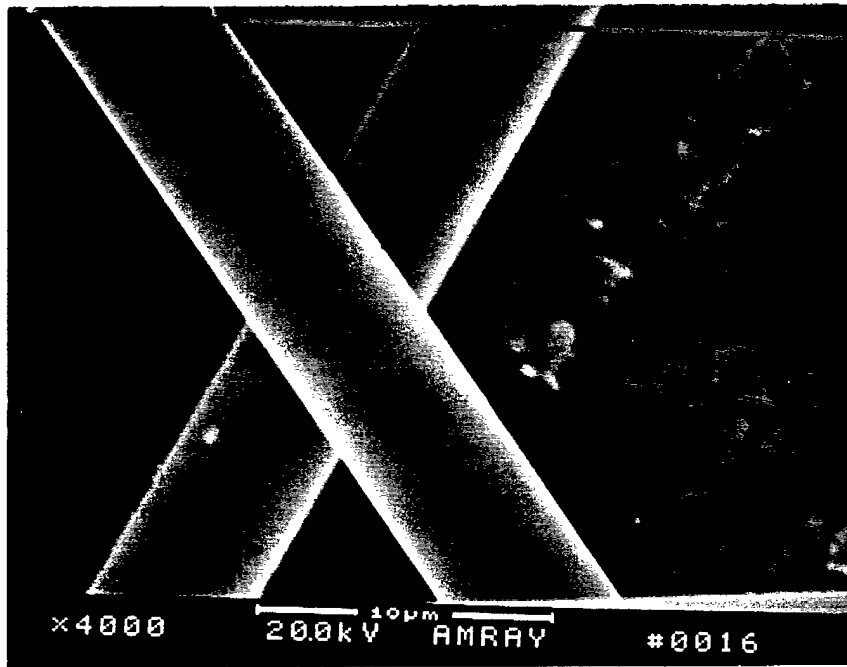


Figure 14. Surface appearance of unsized IM7 fibers

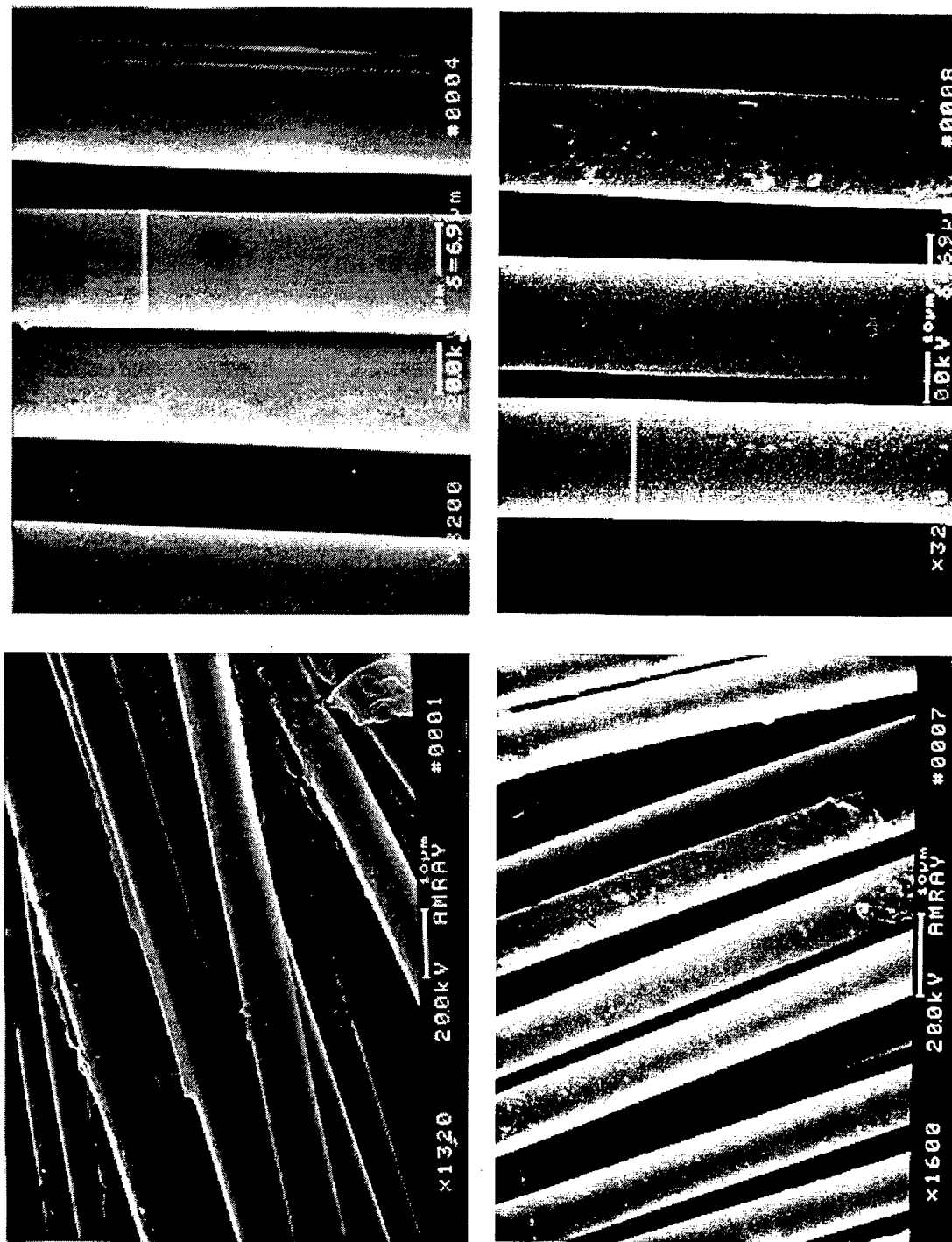


Figure 15. Appearance of finish with AT-CA-9301 coupling agent. Top as-finished. Bottom after 2-hour acetone wash.

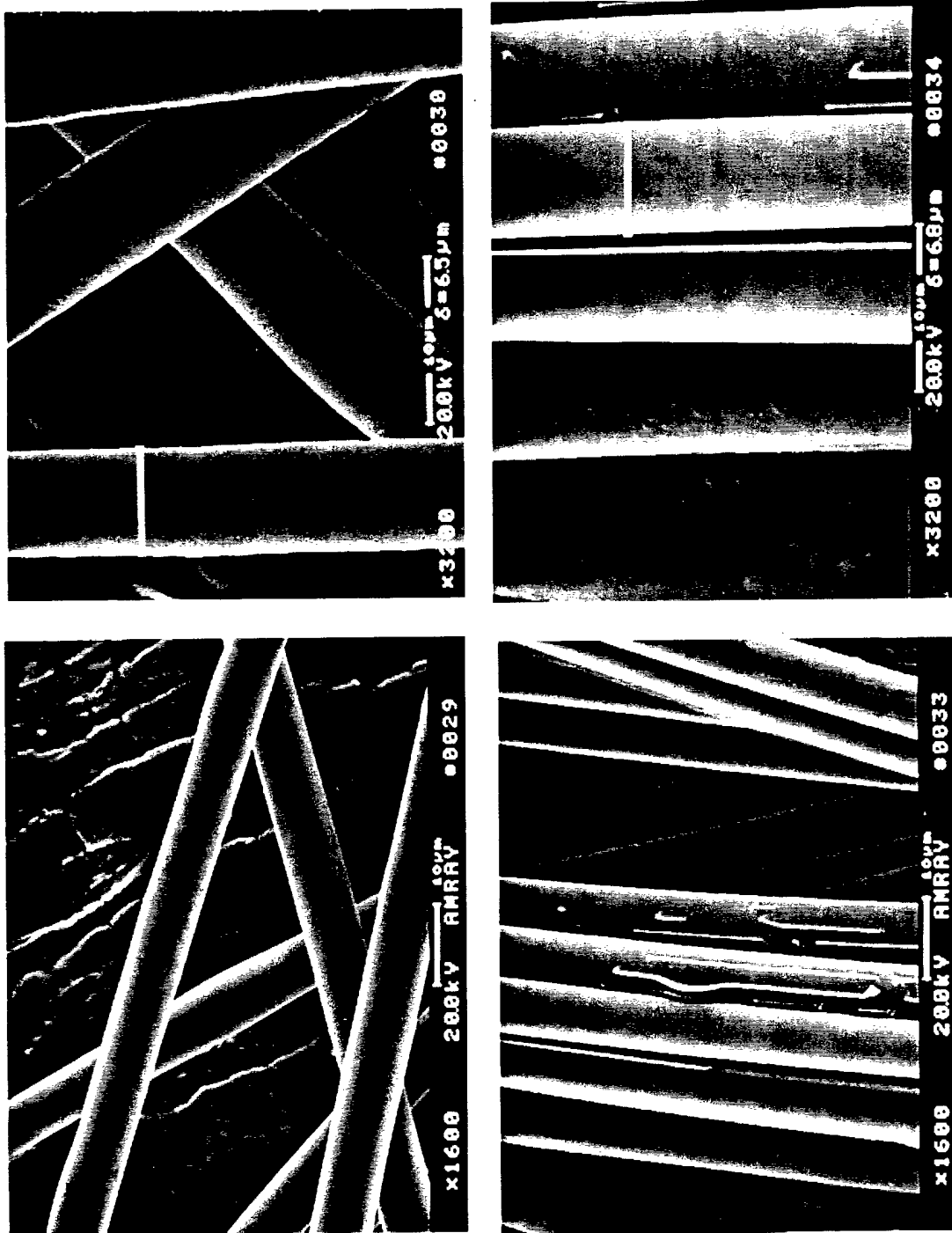


Figure 16. Appearance of finish with AT-CA-9304 coupling agent. Top as-finished. Bottom after 2-hour acetone wash.

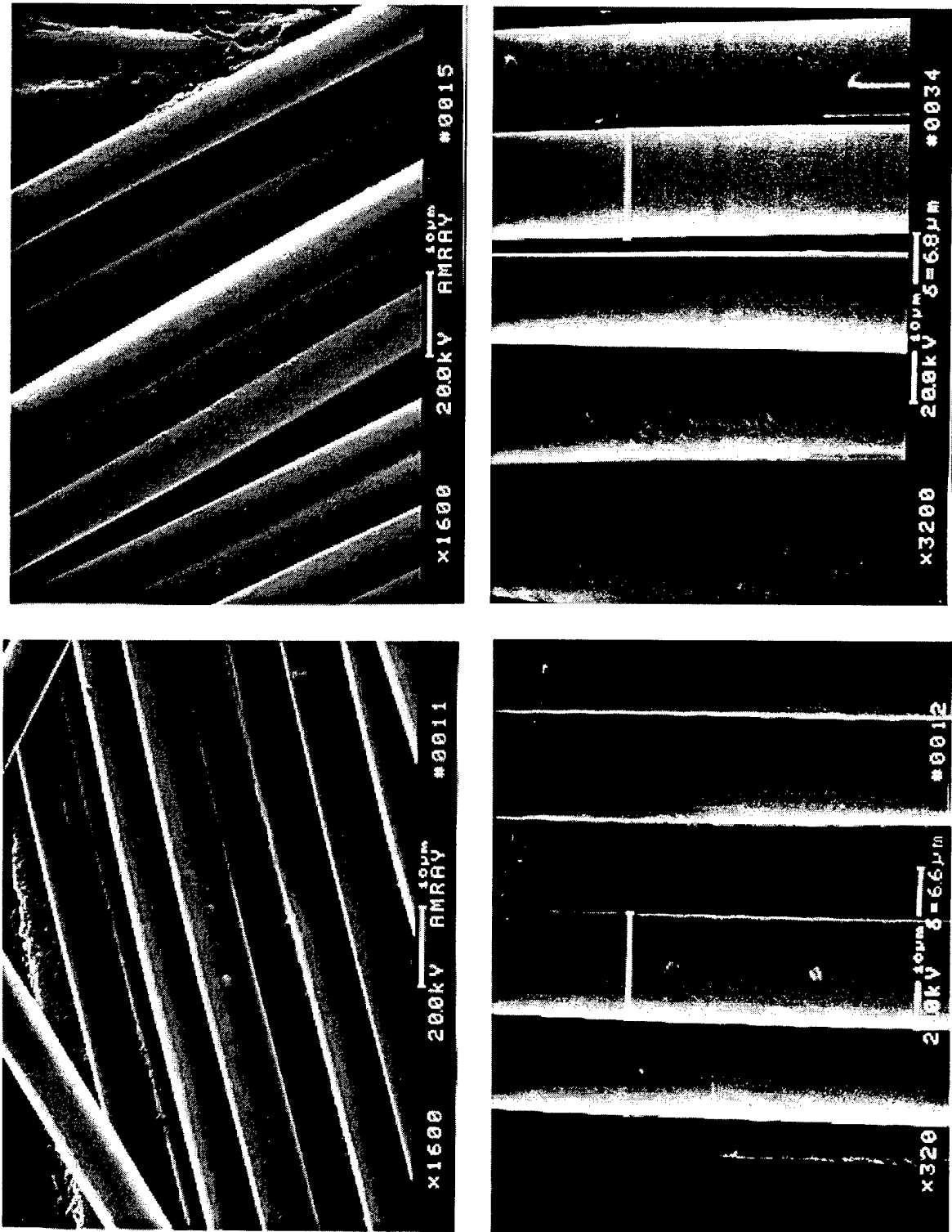


Figure 17. Appearance of finish with AT-CA-9305 (Lot 1) coupling agent. Top as-finished. Bottom after 2-hour acetone wash.



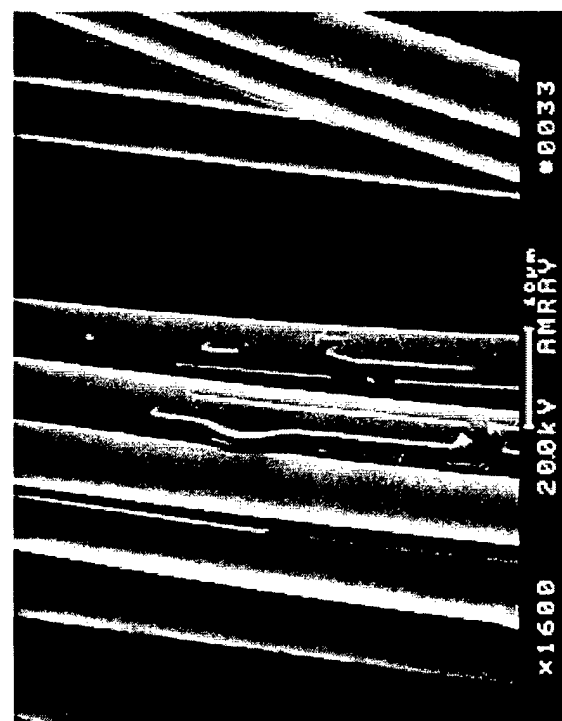
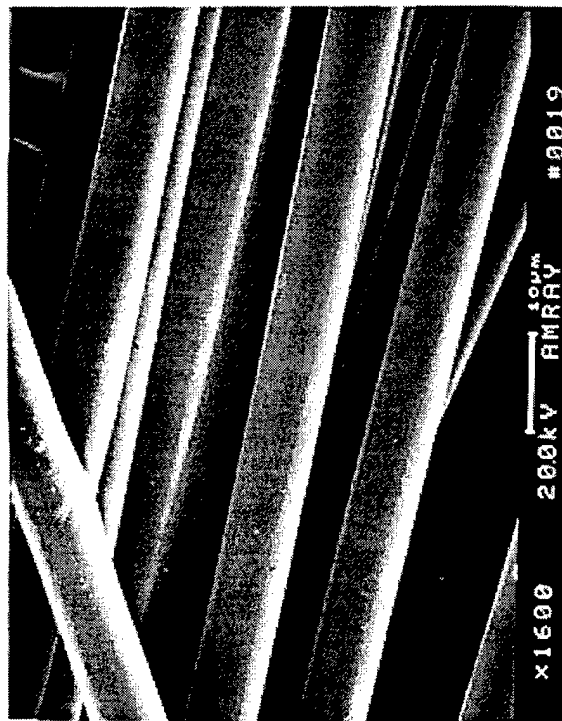
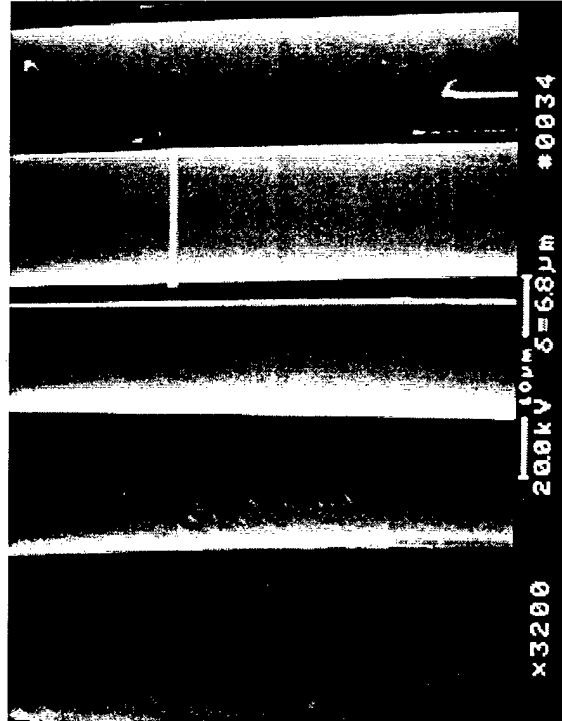
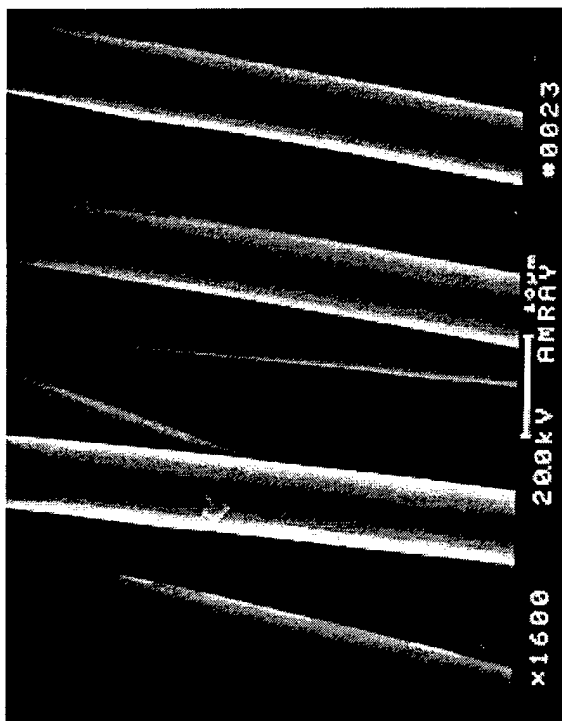


Figure 18. Appearance of finish with AT-CA-9306 coupling agent. Top as-finished. Bottom after 2-hour acetone wash.



SEM observations of finished fibers bent over a 1-mm diameter radius showed no evidence of cracking at coupling agent concentrations up to 1%. This shows that the coupling agent is not embrittling the finish, which could form an undesirable interphase structure.

The SEM observations are very encouraging. In general, the finishes uniformly coated the fiber. All of the finished samples showed evidence of a coating adhering to the fibers even after the 2-hour acetone wash and little polymer was seen in the wash solution. This is taken to mean that all of the coupling agents reacted to form covalent bonds between the fibers and phenolic carrier. Subsequent incorporation of the fibers with grafted phenolic into a BMI matrix composite should result in a more corrosion-resistant material by isolating the BMI from the carbon surface. Based on these results, finishes were applied as 1.0% solutions with 0.1% reactive coupling agent for the majority of the remaining corrosion and composite studies.

### Composite Screening Tests

#### *Voltage Contrast XPS*

Three types of screening tests to measure adhesion and corrosion resistance were run on the 12K tow composite rods before examination of composite plates. Fiber-matrix adhesion was examined using voltage contrast XPS analysis on the BMI matrix rods. Integration of the C<sub>1s</sub> peaks for fiber and matrix and ratioing those results gives an approximate amount of interface-to-matrix cohesive failure in the sample. Spectra from both sides of the specimen were averaged to yield the results given in Table VI.

**Table VI. Voltage Contrast XPS Results on BMI Matrix Rods**

<b>Finish</b>	<b>Carbon Fiber/Carbon Matrix</b>
Unsize	1.45 ± 0.20
PH9301F	0.40 ± 0.15
PH9304F	0.25 ± 0.10
PH9305F	0.90 ± 0.15
PH9306F	1.45 ± 0.15*
*Incomplete signal separation.	



The VC-XPS results in Table I are very encouraging. The lower the carbon fiber contribution to the fracture area, the lower the amount of interface failure present in the sample. These initial results show that the desired carbon-coupling agent bond is occurring. That bond is the difficult link to achieve in tailoring interfacial adhesion. Adhesion controlled by the interphase region can be manipulated by finish composition providing the bond to the carbon surface is attained. The spectrum from the PH9306F sample has a high peak in the  $C_{1s}$  region of the fiber that may not be fiber. As such, those results may be biased against the finish by showing less adhesion than is taking place.

Specimens from the VC-XPS measurements were characterized using SEM. As seen in Figure 19, the unsized, shear-treated IM7 fiber controls provide adequate adhesion in the as-fabricated condition and display a mixed mode (interfacial-matrix cohesive) failure appearance. The finished composites shown in Figures 20-23 display a similar mixed-mode failure with generally a higher degree of matrix cohesive component. The PH9304F finished material shown in Figure 21 has a high degree of cohesive failure, while the other finish compositions are quite similar in appearance. These results follow the basic trend of the VC-XPS data given in Table V and reinforce those results.

### *Galvanic Corrosion*

The second screening tests examined galvanic corrosion susceptibility. The appearance of the sample rods after 2 days of immersion is shown in Figure 24. Little aluminum corrosion product was seen with the PH9301F and PH9304F finishes shown in 24a and 24b. A small amount of corrosion product is seen with the PH9306F finish (24c) and a larger amount with the PH9305F finish (24d). The control samples (24e and f) exhibited a similar amount of corrosion product as the PH9305F sample.  $Al(OH)_3$  is the expected corrosion product.

The galvanic corrosion test was continued for 14 days total exposure. This amount of exposure is severe enough to screen the finish performance. Upon removal from the salt water, the composite samples were washed with distilled water 3 times, patted dry, and weighed. The weight changes observed are shown in Figure 25. The PH9301F-finished samples showed an average weight loss, while the PH9304F and PH9306F-finished samples showed a small weight gain and the PH9305F-finished and control samples showed a larger average weight gain. Weight gains should be due to moisture absorption and weight losses to degradation of the BMI matrix. It is likely that the samples showing weight gains have absorbed a larger amount of water, which may indicate additional matrix and interface degradation creating paths for the ingress of water.

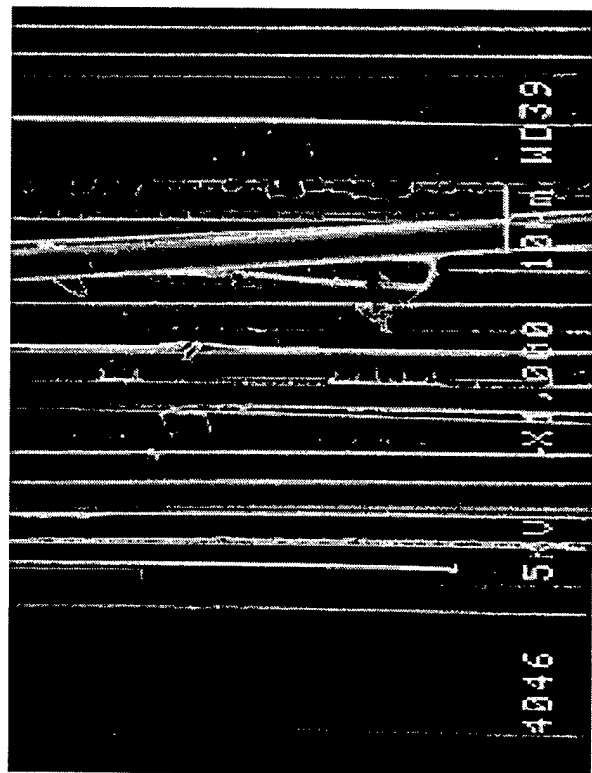
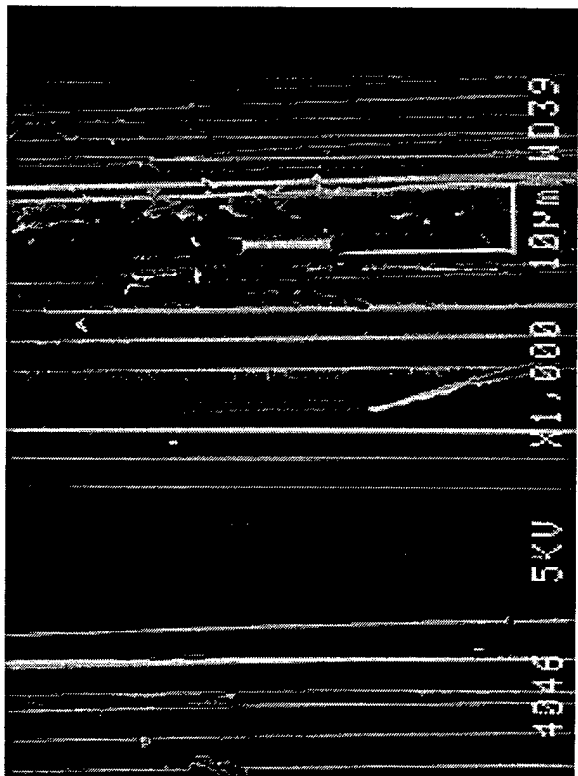
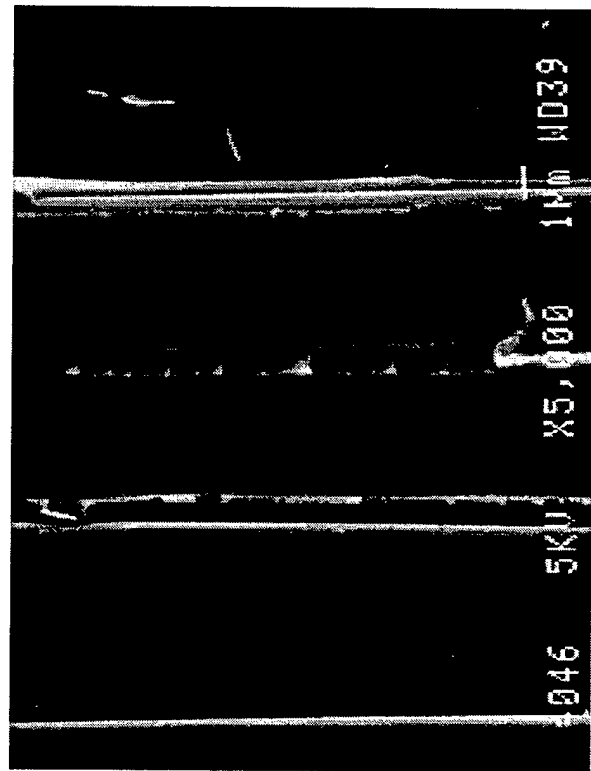
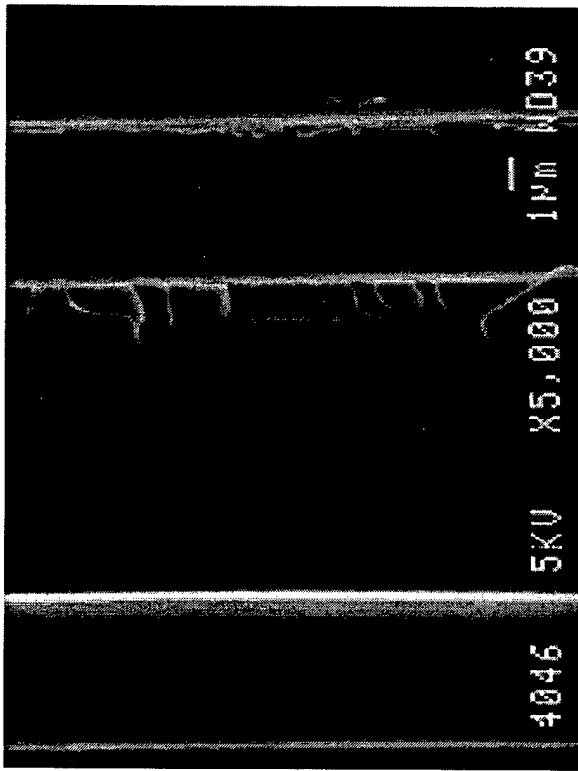


Figure 19. Fracture surface appearance of unsized IM7/BMI composite

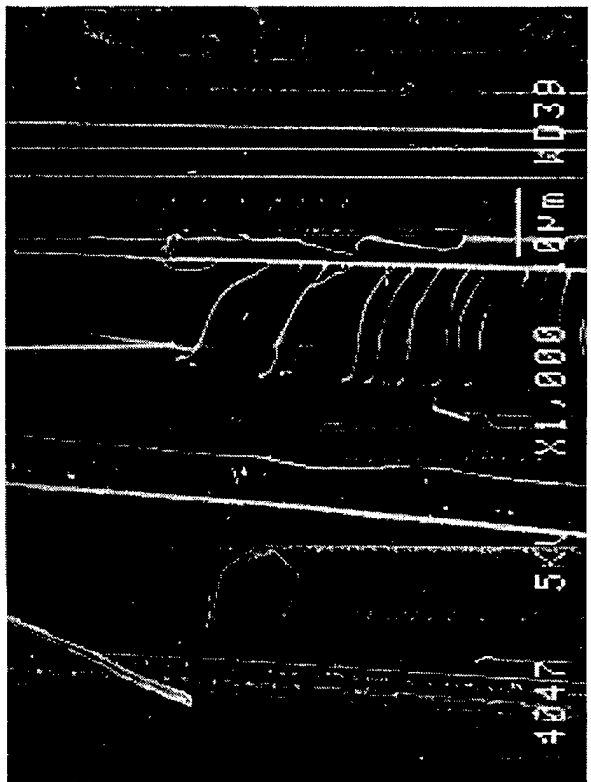
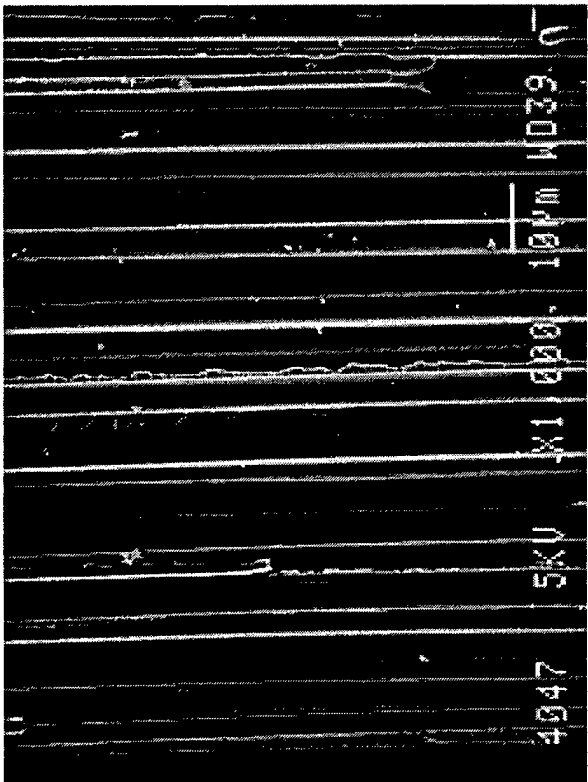
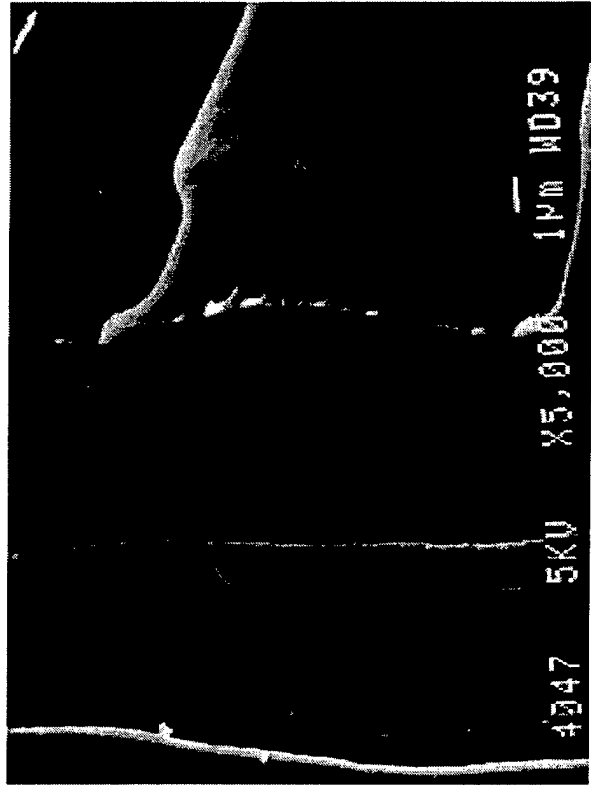
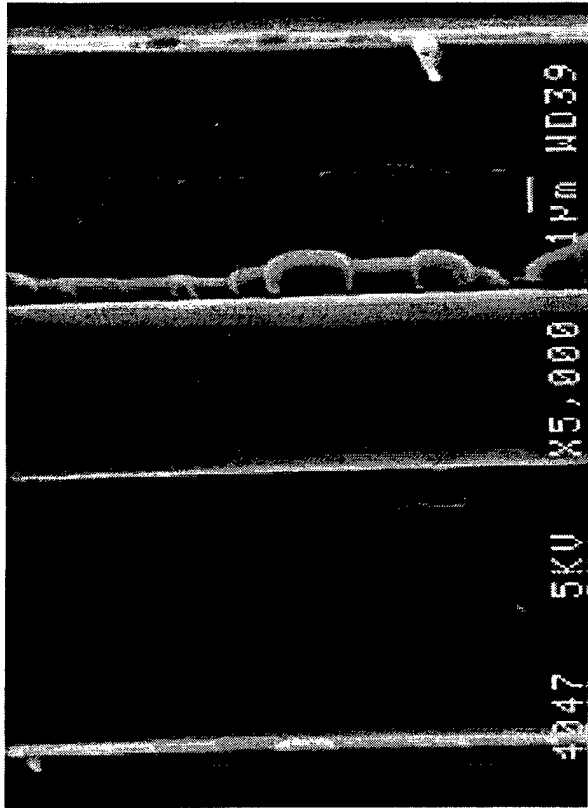


Figure 20. Fracture surface appearance of IM7/BMI composite with PH9301F finish

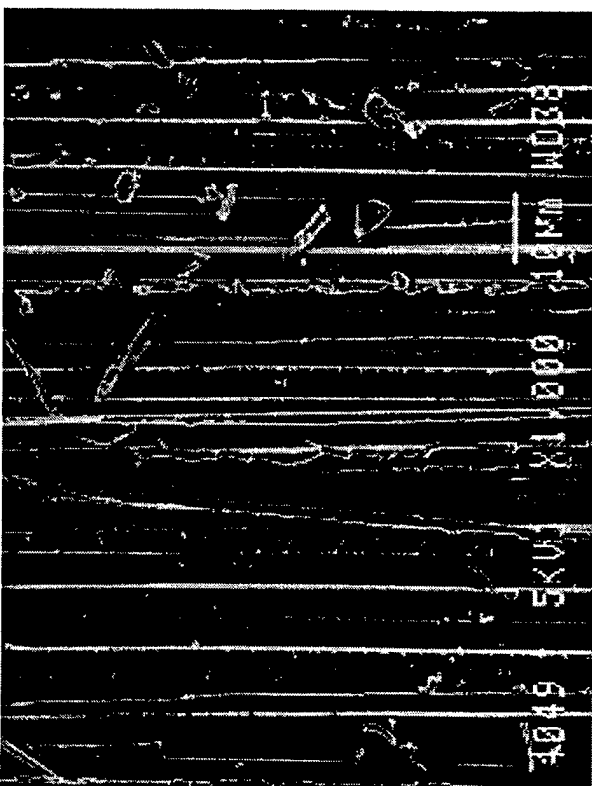
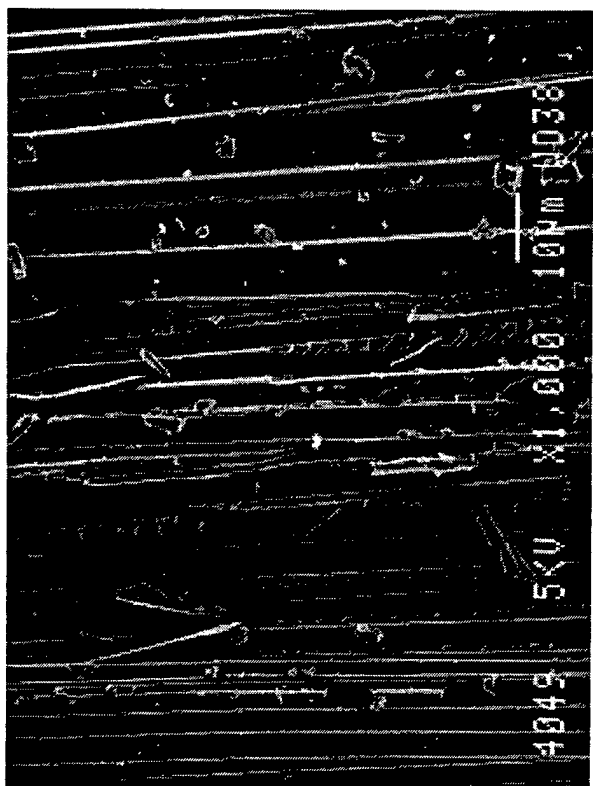
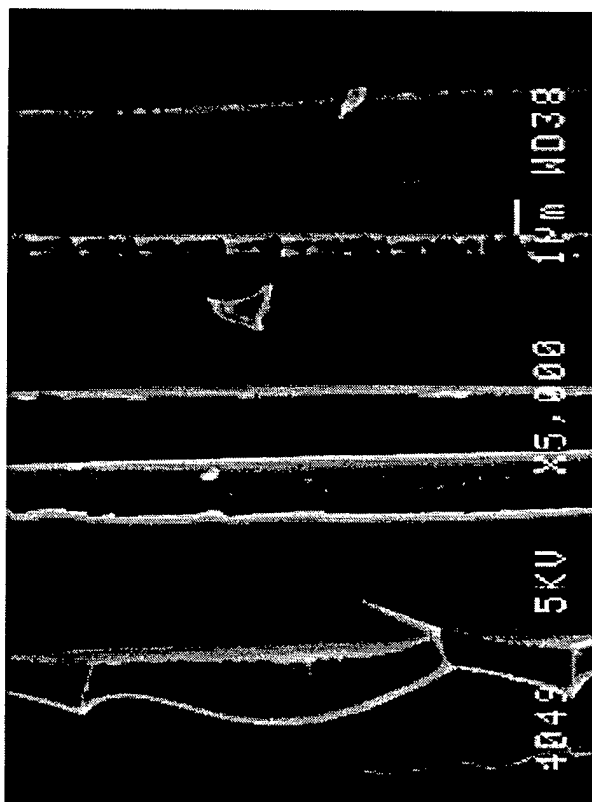
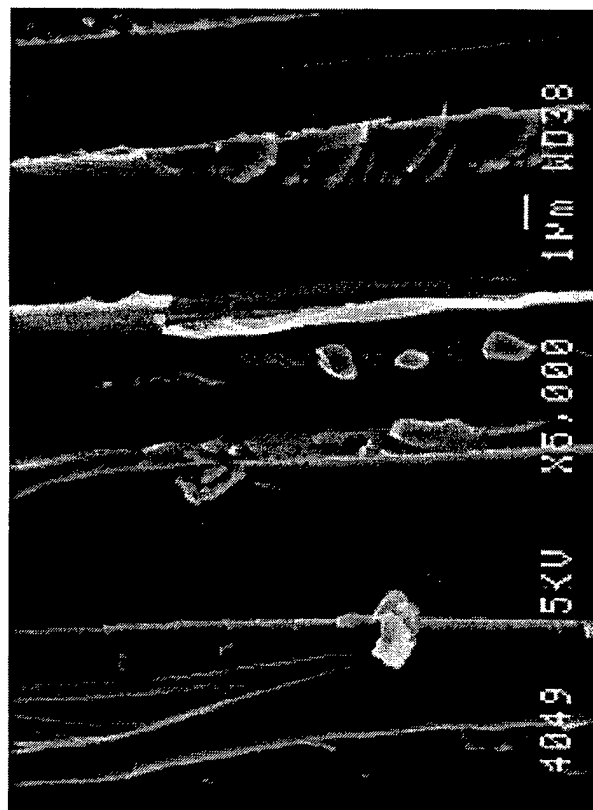


Figure 21. Fracture surface appearance of IM7/BMI composite with PH9304F finish

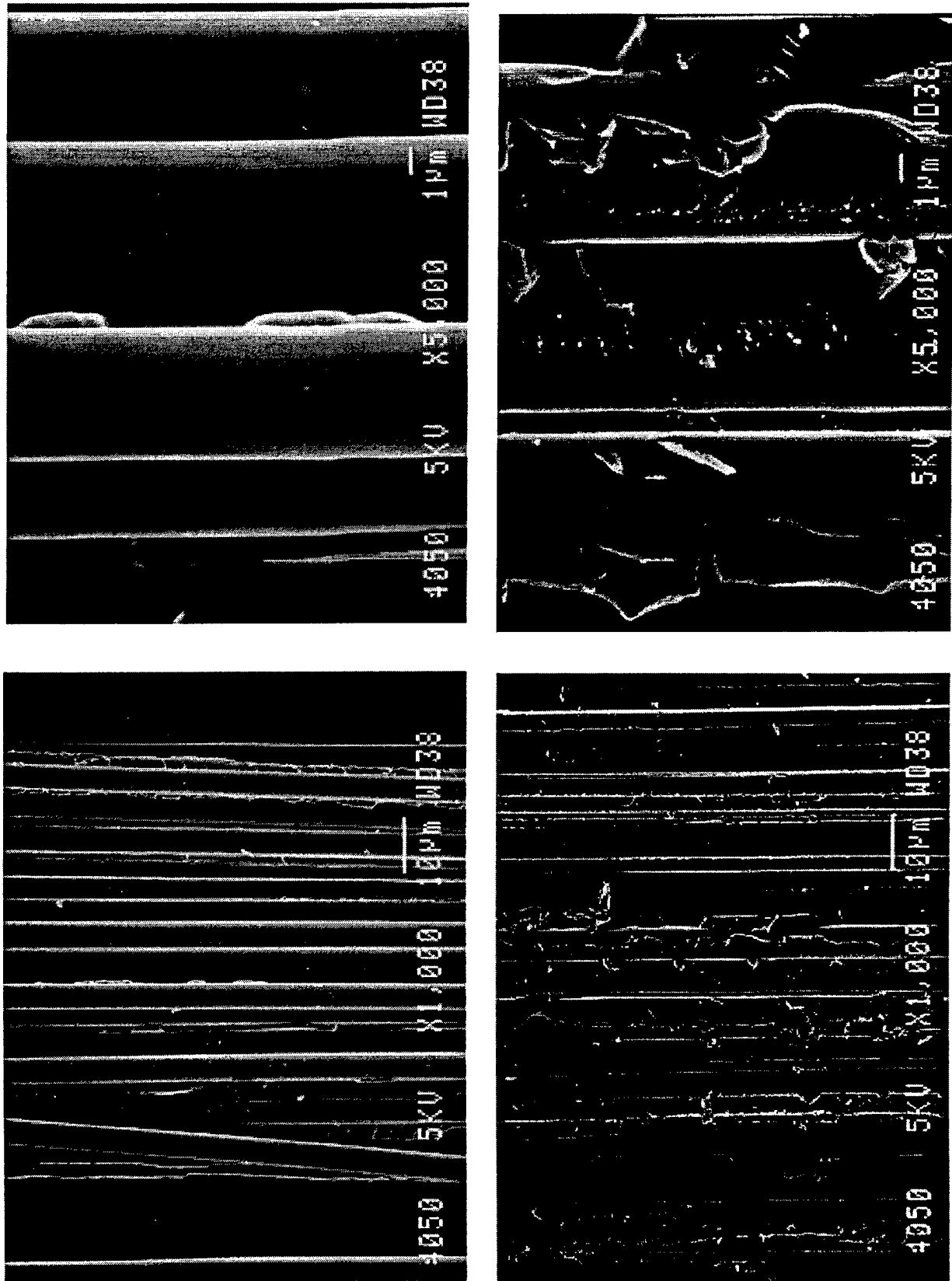


Figure 22. Fracture surface appearance of IM7/BMI composite with PH9305F finish

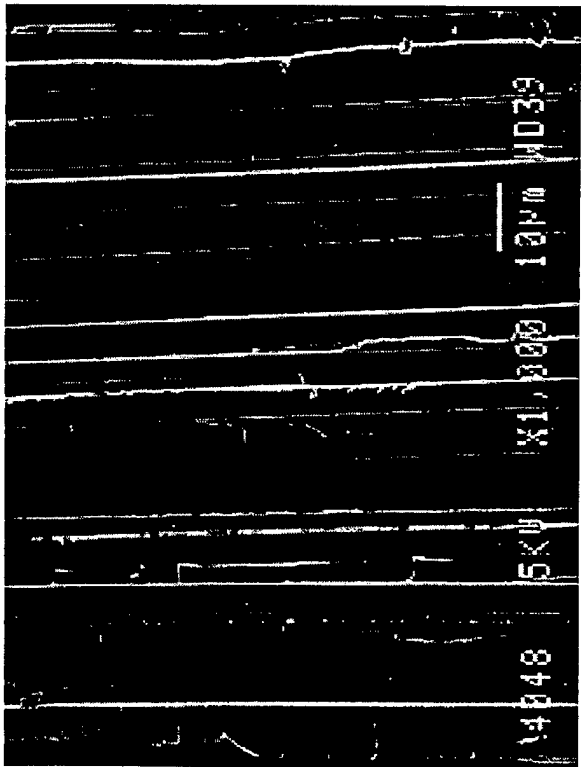
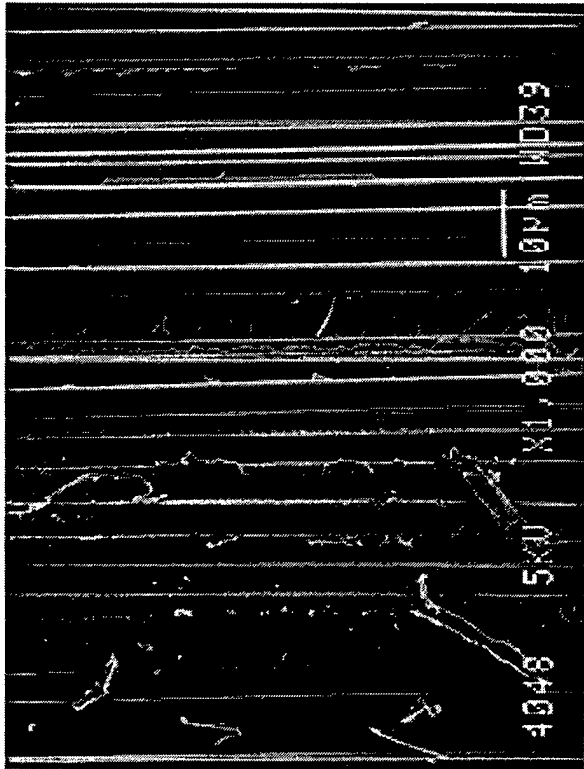
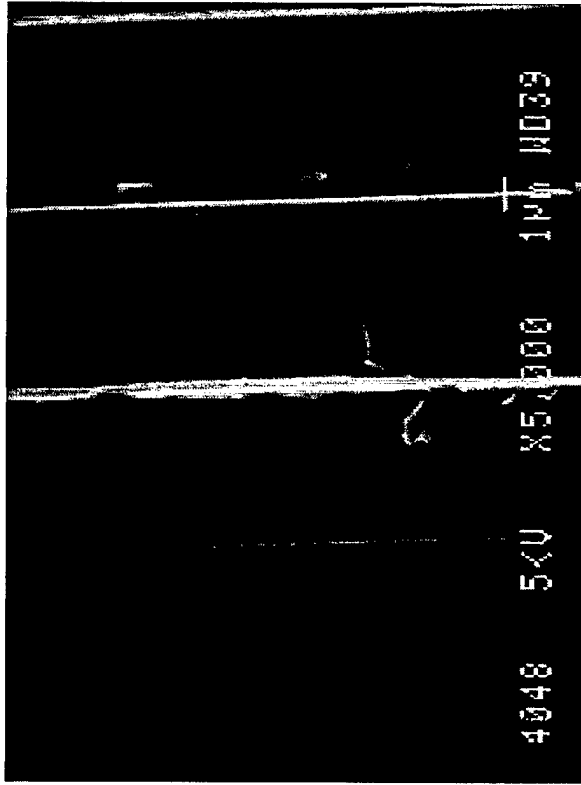
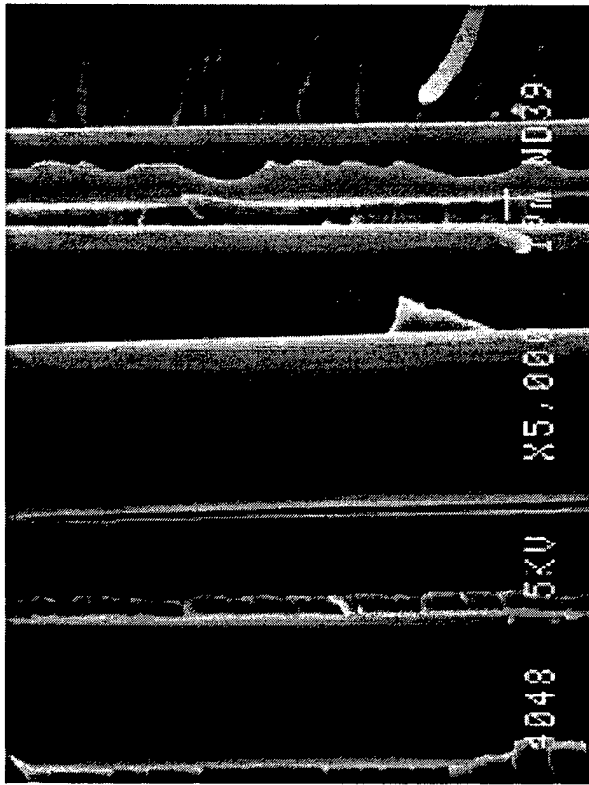
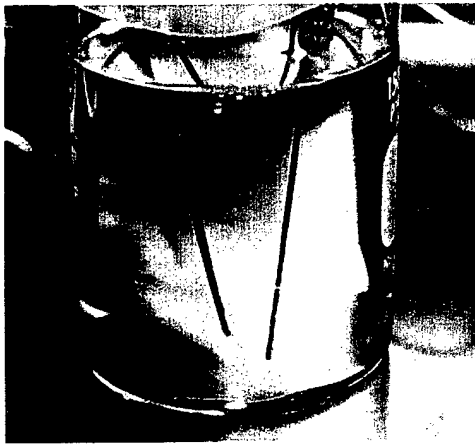
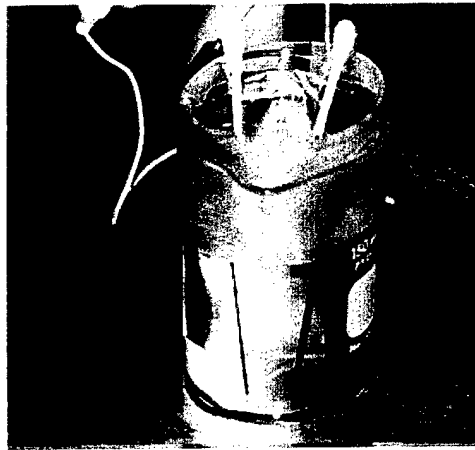


Figure 23. Fracture surface appearance of IM7/BMI composite with PH9306F finish

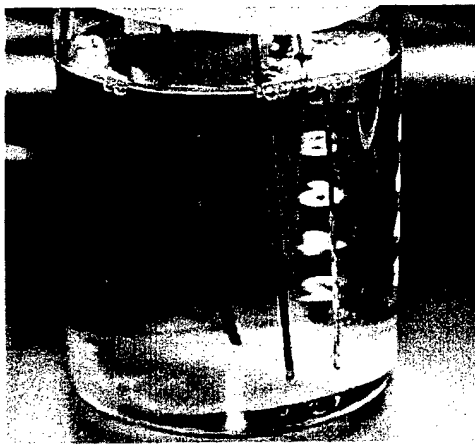




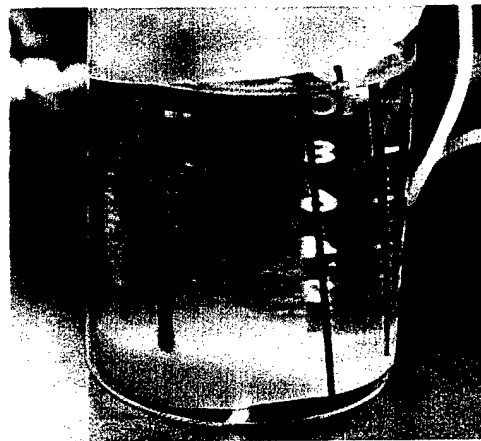
a) 9301 Finish



b) 9304 Finish



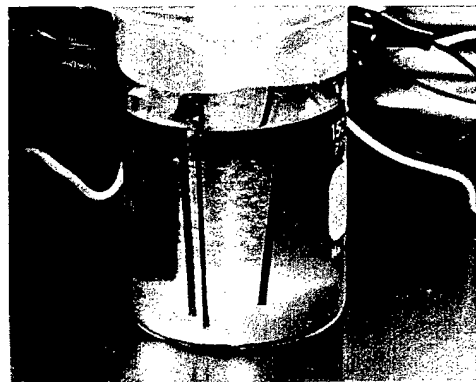
c) 9306 Finish



d) 9305 Finish



e) Control Sample 1



f) Control Sample 2

Figure 24. Galvanic corrosion samples after 2 days of immersion

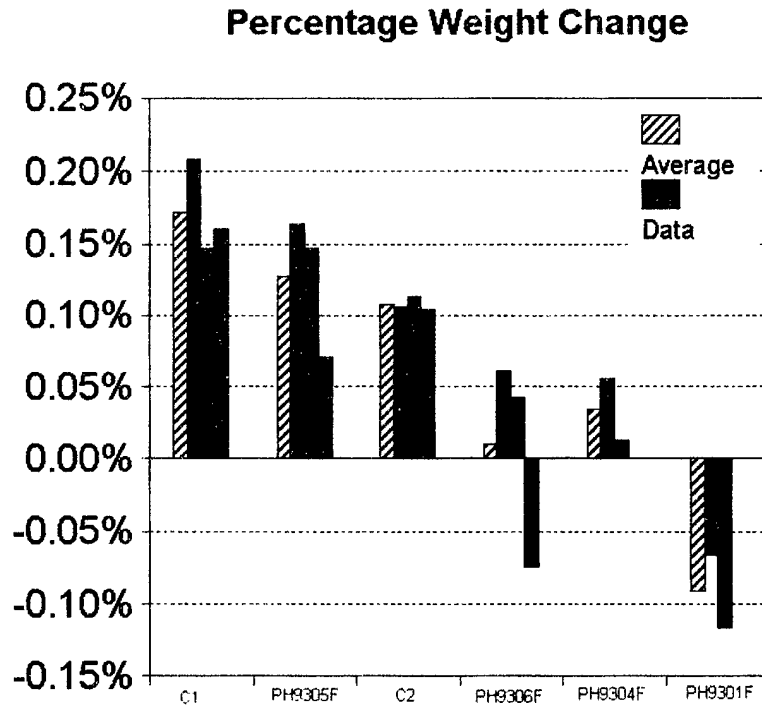


*Figure 25. Weight changes after 2 weeks of immersion*

The specimens from the galvanic couple corrosion experiments with BMI matrix composite rods were characterized using SEM. The surface appearance of the corroded specimens was examined slightly above and below and at the water line. In general, more degradation of the BMI was observed at and above the water line on all specimens, but trends between sample types were the same for each location. For comparison of the unsized and finished materials, the appearance above the water line will be used in the following discussion. All specimens were washed thoroughly in distilled water before examination.

The appearance of the unsized control specimens after 14 days exposure is shown in Figure 26. A low magnification view of the control specimen surface in Figure 26a shows a variation between exposed largely clean fibers and areas where the BMI matrix is degrading. A higher magnification view of the degrading resin shown in Figure 26b reveals a rough texture for the remaining resin. The texture seen in Figure 26b could also be deposited salts that were not removed by the washing step although only control specimens displayed this type of texture.

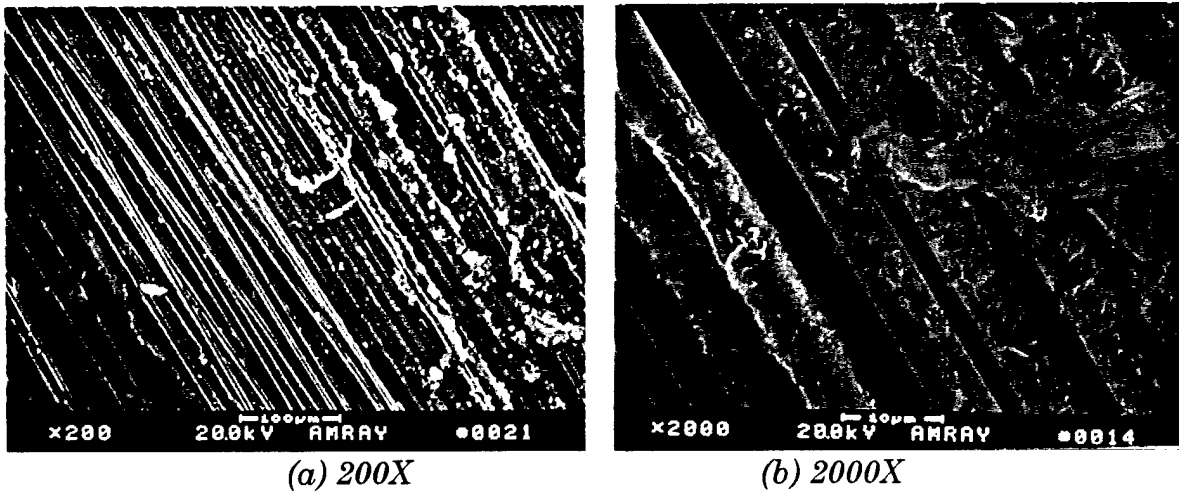
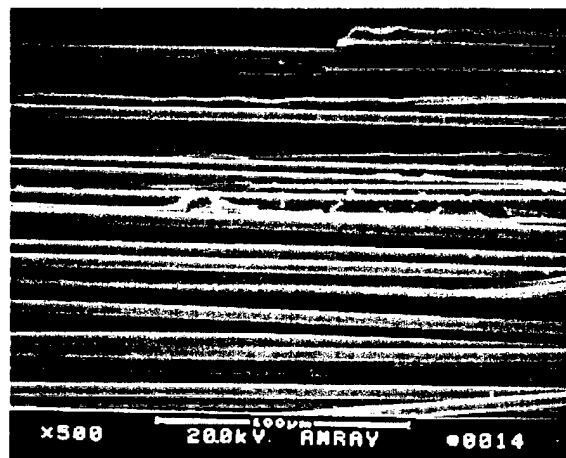
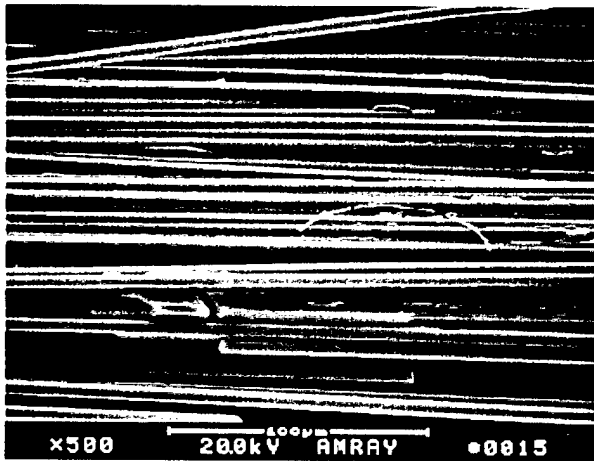


Figure 26. Surface appearance of unsized IM7/BMI control corrosion specimens

The finished specimens showed varying degrees of resin degradation, all less than the unsized controls. Surface appearance of the finished specimens is shown in Figures 27-30. The PH9301F (Figure 27) and PH9304F (Figure 28) finished samples have most of the BMI resin intact and show the beginning of resin degradation exhibited in cracking and delamination. Both the PH9305F (Figure 29) and PH9306F (Figure 30) finished specimens show the BMI resin delaminating and peeling from the composite in long strips in areas of the surface. Other areas show the resin intact. Higher magnification views show the delamination process beginning (Figure 29) and only a small amount of resin remaining in the delaminated regions with the PH9306F finish (Figure 30).

Figure 27. Composite surface appearance with PH9301F finish after galvanic exposure (500X)



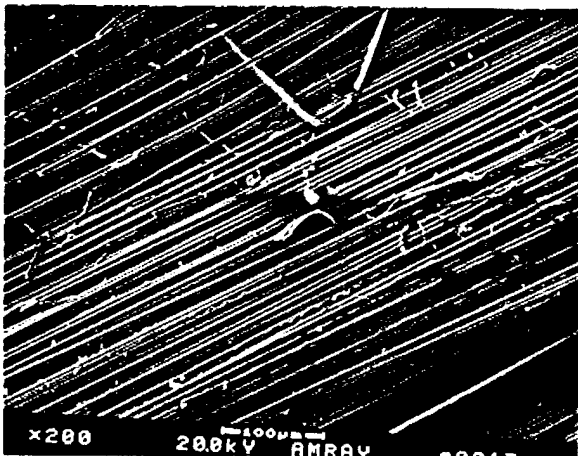


(a) 500X

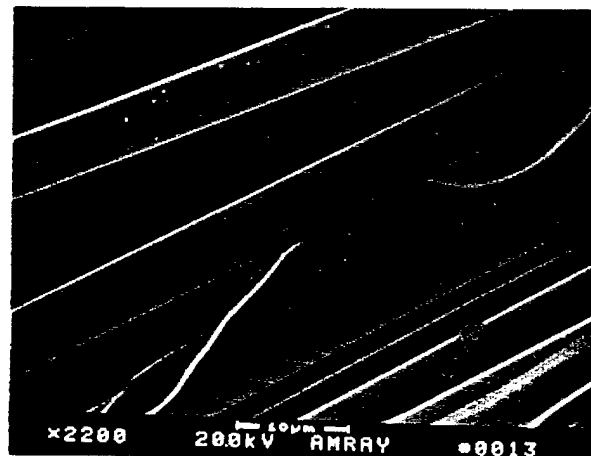


(b) 2000X

Figure 28. Composite surface appearance with PH9304F finish

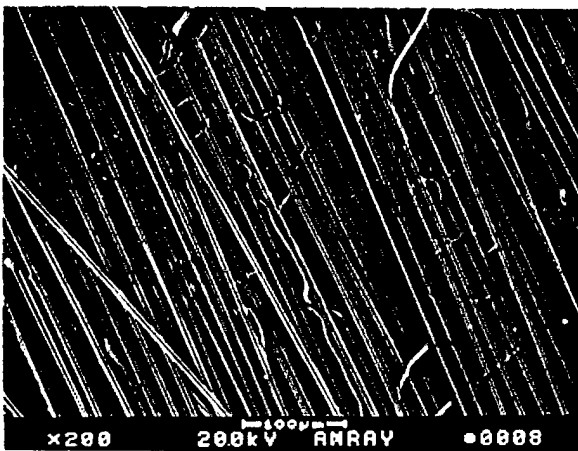


(a) 200X

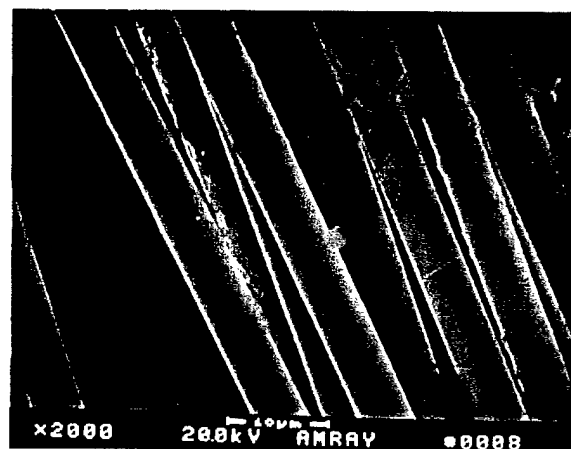


(b) 2000X

Figure 29. Composite Surface appearance with PH9305F finish



(a) 200X



(b) 2000X

Figure 30. Composite surface appearance with PH9306F finish



Examination of the composite surface structure at and below the water line in the galvanic cell shows the unsized material to be severely degraded displaying a unique texture as shown in Figure 31.

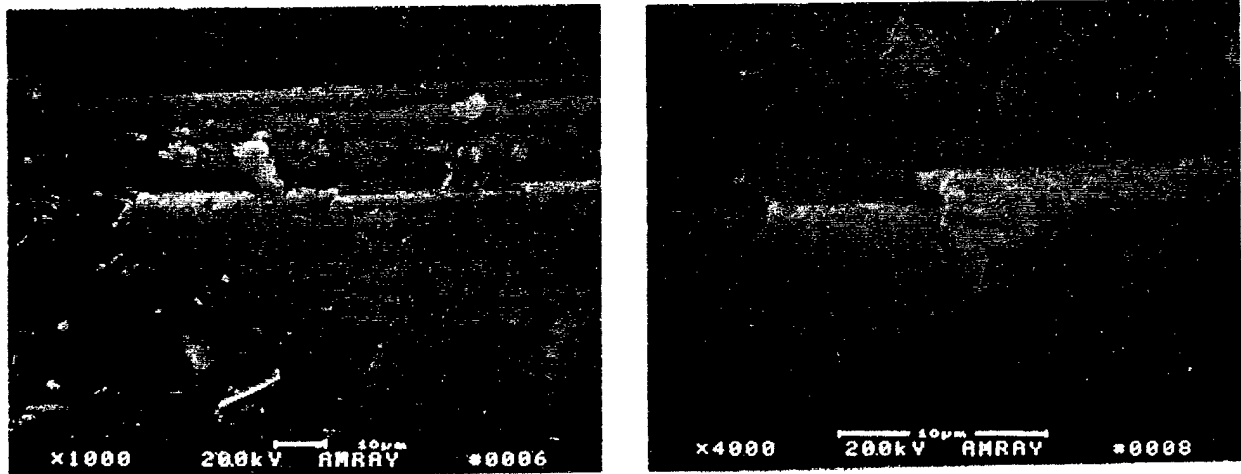


Figure 31. Surface appearance of unsized composite below water line

In contrast, the surface of the finished materials below the water line show only some cracking and beginning of delamination as shown in Figure 32.

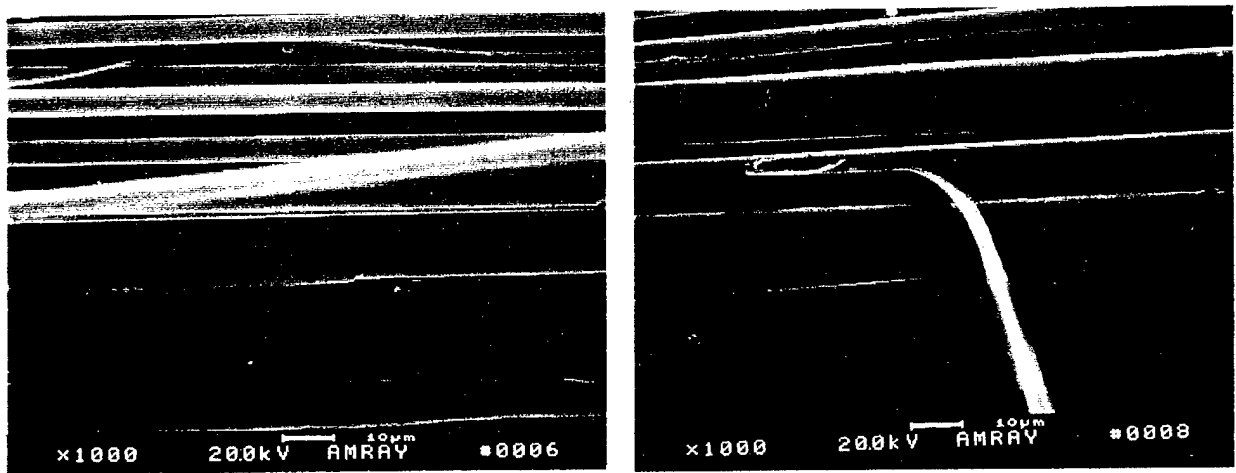


Figure 32. Surface appearance of PH9304F finished composite below water line

Additional insight into the protection from BMI galvanic corrosion afforded by the reactive finishes can be gained by examination of the extent of corrosion of the aluminum anodes. Uncoupled aluminum in the salt solution showed no evidence of attack. The appearance of the aluminum base of the control (unsized composite) couple is shown in Figure 33. The aluminum electrode shows a substantial amount of attack in the corrosion process and has decoupled from the upright leg of the L-shaped anode. In contrast, the anodes of the PH9301F and PH9304F finished



specimens show only a small amount of aluminum corrosion and no evidence of attack at the bend leading to the upright portion (Figures 34 and 35). The anodes of the couples with the PH9305F (Figure 36) and PH9306F (Figure 37) specimens show an increasing amount of corrosion, but still substantially less than the controls. These observations follow the trends seen in weight changes presented in Figure 25 and the VC-XPS results for adhesion given in Table VI.

*Figure 33. Appearance of aluminum anode coupled to unsized control composite*

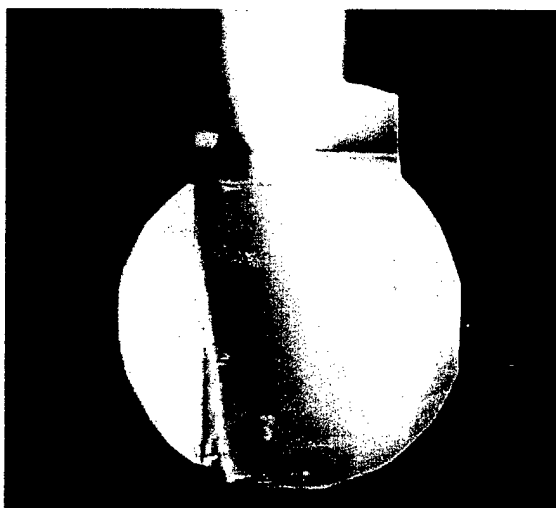


*Figure 34. Appearance of aluminum anode coupled to PH9301F finished composite*



*Figure 35. Appearance of aluminum anode coupled to PH9304F finished composite*

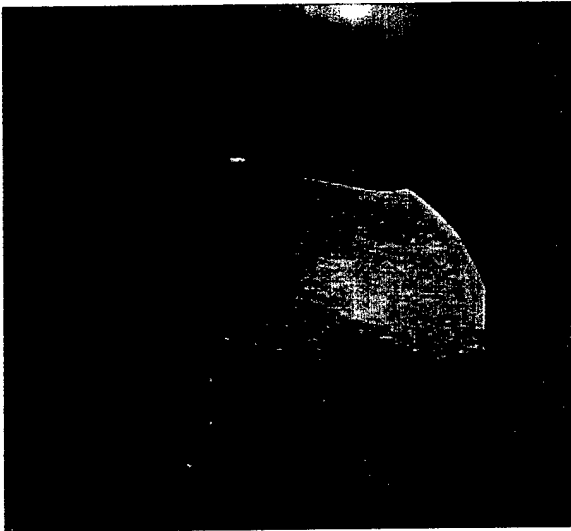
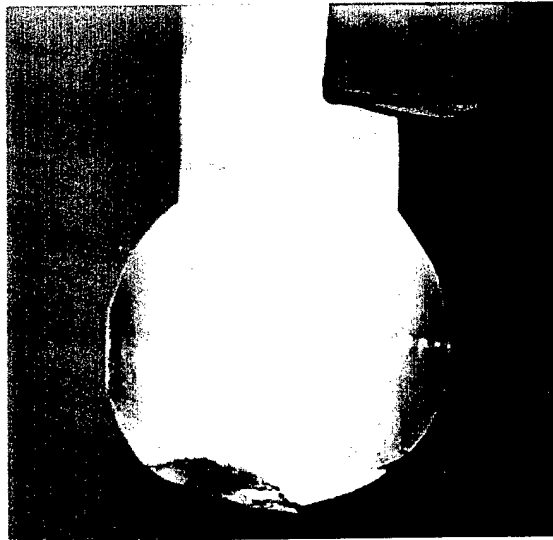
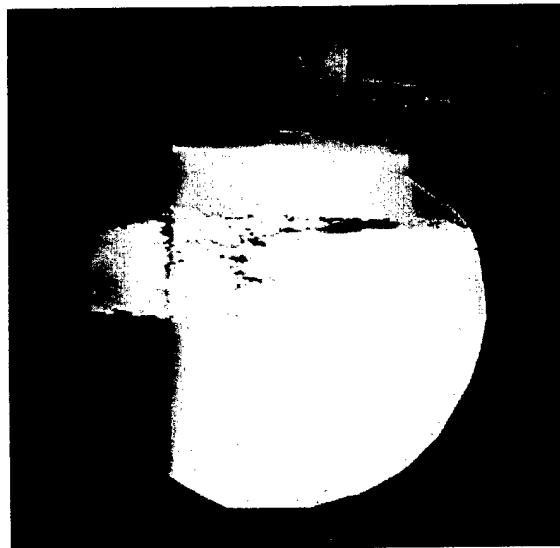


*Figure 36. Appearance of aluminum anode coupled to PH9305F finished composite*

*Figure 37. Appearance of aluminum anode coupled to PH9306F finished composite*





### **Electrochemical Impedance Spectroscopy (EIS)**

The third screening test on the 12K tow composites used electrochemical impedance spectroscopy (EIS). The EIS experiments were run on duplicate sample rods fabricated for the static corrosion experiments. Following the baseline measurements, a capacitance was calculated that corresponds to the area of exposed carbon in the composite. The debonded area is calculated by dividing the measured capacitance by  $20\mu\text{F}/\text{cm}^2$ , which is an accepted value for the interfacial capacitance for carbon/graphite in aqueous solutions. The samples were then subjected to cathodic polarization for 1 hour at -1.4V and the impedance rerun. Results are given in Table VII.

**Table VII. Calculated Debonded Area from EIS Measurements**

<b>Finish</b>	<b>Initial Debond Area (cm<sup>2</sup>)</b>	<b>Final Debond Area (cm<sup>2</sup>)</b>
PH9301F	0.01	0.70
PH9304F	0.02	0.74
PH9305F	0.02	0.90
PH9306F	0.09	2.13
Control	0.147	1.05

The initial complex impedance corrosion data given in Table VII are somewhat encouraging from an optimistic point of view in that most of the finished composites performed better than the controls.

Taken together, the corrosion and adhesion data on the 12K rods suggest that all the finishes except the PH9306F provide improved adhesion and galvanic corrosion protection for BMI-matrix composites.

### **Composite Mechanical Properties**

Following the screening tests on 12K tow rods, composite panels were prepared with each finish and an unsized control. Specimens from the composite panels were tested for longitudinal flexural strength and short beam shear strength. A concern with the approach being taken to isolate the BMI with a thick finish coating is that a second weak interface can be created at the finish-BMI interface. That would not be evident from any of the screening tests discussed above including the VC-XPS if





the finish is well bonded to the carbon fiber. Results from mechanical property screening tests are given in Figures 38 and 39.

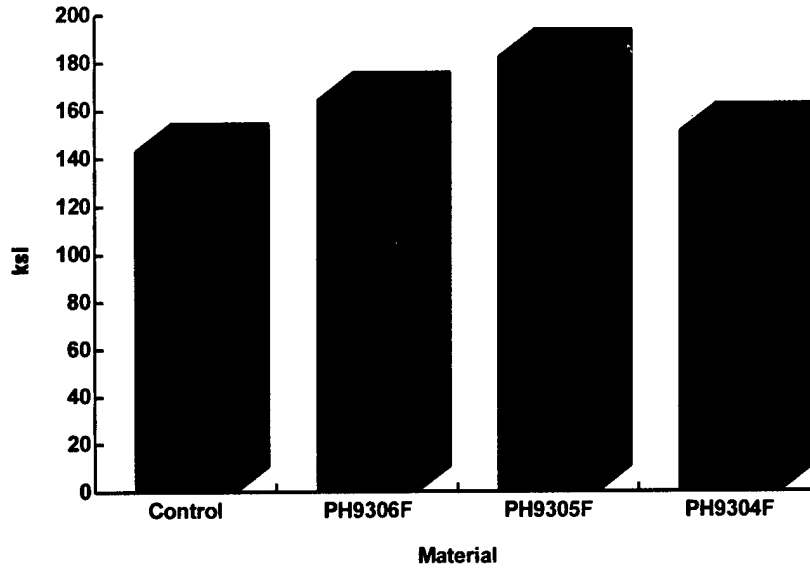


Figure 38. Room temperature longitudinal flexural strengths for IM7/BMI composites

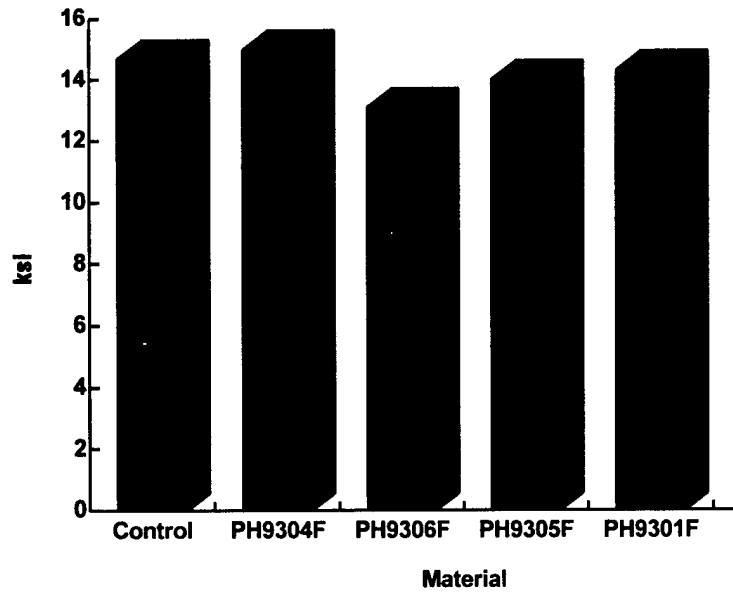


Figure 39. Room temperature short beam shear strengths for IM7/BMI composites



With the exception of the low SBS strength of the PH9306F finished material, the mechanical properties of the finished composites are in the same range as the unsized control. This shows that the phenolic finish is not creating a weak interface with the BMI matrix, which shows that reactive finishes can be a practical approach to prevent galvanic corrosion in the BMI-matrix carbon composite.

Following the flexure and short beam shear screening tests, the PH9304F finished material and an unfinished control were selected for more in-depth mechanical property evaluation. Those tests included elevated temperature testing with and without moisture and compression testing in addition to 0 and 90 degree flexure and short beam shear. Results of those tests are summarized in Table VIII.

**Table VIII. Mechanical Properties of BMI Matrix Composites**

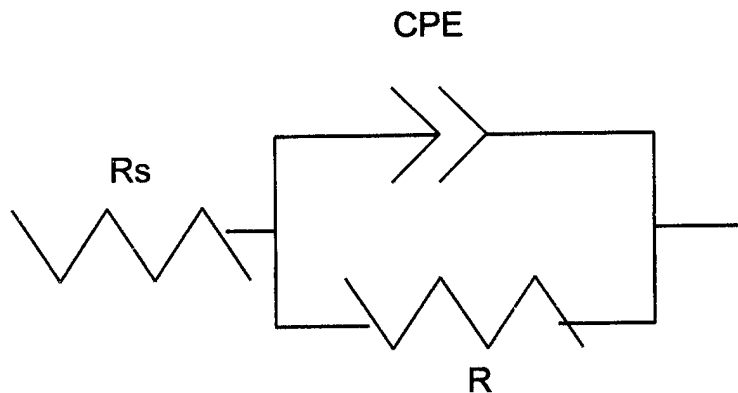
Composite	Test Condition (°C)	Fiber Orientation (degrees)	Flexural Strength (ksi)	SBS Strength (ksi)	Compressive Strength (ksi)
Control	23	0	144.7 ± 7.2	11.5 ± 0.7	128.8 ± 16.4
		90	8.4 ± 0.5	--	--
	177	0	11.3 ± 6.9	--	--
		90	7.8 ± 1.4	--	--
	177/wet	0	81.9 ± 5.2	--	--
		90	3.9 ± 1.6	--	--
PH9304F	23	0	151.4 ± 4.1	11.1 ± 0.7	190.1 ± 17.6
		90	6.1 ± 1.5	--	--
	177	0	112.0 ± 4.1	--	151.0 ± 6.8
		90	7.0 ± 0.8	--	--
	177/wet	0	73.7 ± 2.4	4.2 ± 0.5	--
		90	1.6 ± 0.3	--	--



Examination of the results given in Table VIII shows that the finished material in general has similar properties to the unfinished control. The finished panel has higher compressive properties but shows more sensitivity to hot-wet conditions in this limited test matrix. Additional work is required to determine the nature of the hot-wet response and potential means of improving that response in the finished material.

### Electrochemical Impedance Spectroscopy (EIS)

EIS was run on samples machined from the composite plates. The EIS data were analyzed to extract capacitance values, which were used to determine the relative amount of disbondment produced by cathodic polarization. EIS data were fitted to an equivalent circuit model using a complex non-linear least squares fitting routine. The electrical model used for fitting was as follows:



In this model  $R_s$  accounts for the resistance of the test solution,  $R$  accounts for the charge transfer resistance associated with electrochemical processes occurring on the carbon fiber surfaces. The element termed "CPE" is essentially an imperfect capacitor which accounts for the double layer capacitance that exists at the carbon fiber surfaces. An effective capacitance can be calculated according to:

$$C = Y^{1/n} R^{1-n/n} \tag{1}$$

where  $C$  is the effective capacitance,  $R$  is the charge transfer resistance,  $Y$  is the magnitude of the impedance associated with the imperfect capacitor and  $n$  is a value that describes the deviation from ideal  $1/\omega$  capacitive response.

Changes in the values for the elements in the equivalent circuit model are examined to determine the extent of cathodic disbondment in these experiments. The measured imperfect capacitance is given by:

$$Y(\omega) = \epsilon(\omega)\epsilon_0 A/t \tag{2}$$

and the resistance is given by



$$R = \rho/A \tag{3}$$

where  $\epsilon$  is the double layer capacitance,  $\epsilon_0$  is the permittivity of free space and  $\rho$  is the area specific resistivity for charge transfer on the carbon fiber surface. As disbondment occurs  $Y$  should increase,  $R$  should decrease and  $n$  should decrease. The net effect should be an increase in capacitance with increasing disbondment. By comparing capacitance values before and after cathodic polarization a relative degree of damage should be possible.

Figure 40 shows capacitance versus time responses for the composite samples exposed along the fiber lengths. A control sample containing no surface finish was tested for comparison. Measured capacitance does not significantly increase for the PH9301F, PH9304F, and PH9305F finishes indicating that excellent resistance to cathodic disbondment is conferred. Significant increases in capacitance are detected for the control sample and PH9306F showing that disbondment proceeds in a much more rapid fashion. The fact that the PH9306F curve is nearly identical to that for the control sample indicates that no beneficial effect is derived from the use of this finish.

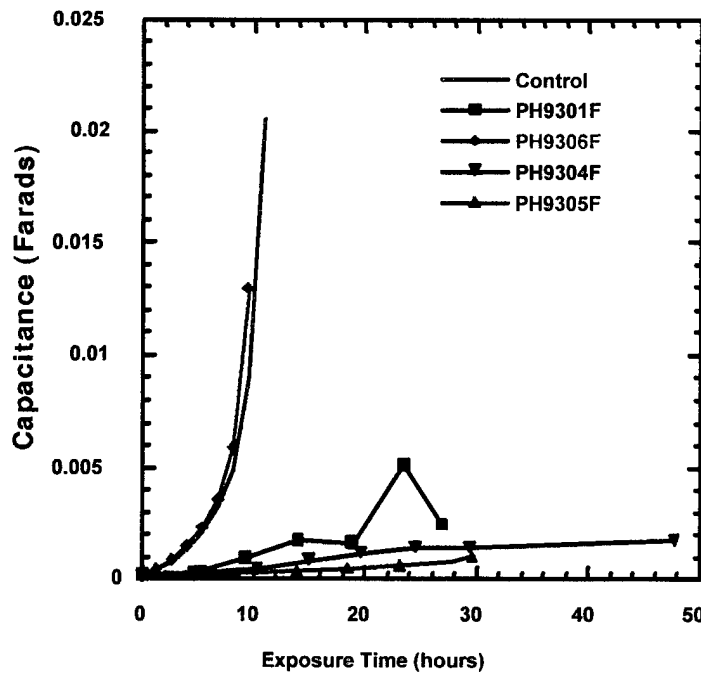


Figure 40. Sample capacitance versus exposure time for control and coupling agent modified composite samples tested to expose fiber lengths

The calculated debonded area from the EIs measurements before and after cathodic polarization is given in Table IX for the longitudinal specimens.



Table IX. Calculated Debonded Area for Longitudinal EIS Measurements

Fiber Finish	Exposure Time (hours)	Area at t = 0 h (cm <sup>2</sup> )	Area at t = exposure time (cm <sup>2</sup> )
unsized	9.6	6.5	450
PH9301F	9.3	7.0	45
PH9304F	10.4	4.0	2.2 (possible swelling)
PH9305F	9.0	6.0	12.5
PH9306F	9.5	7.5	650

Figure 41 shows capacitance versus time curves obtained from the “end-on” test configuration. These data corroborate those shown in Figure 40 (PH9306F not included) showing that the effect of the finishes on cathodic disbondment operates independent of orientation and that the effect is significant enough to be observed in these aggressive types of tests. The calculated debond area for the end-on EIS measurements is given in Table X.

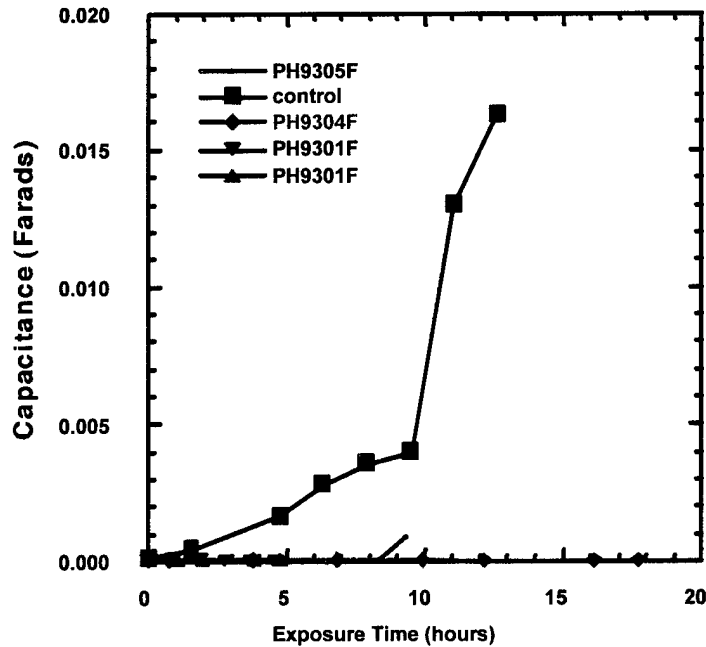


Figure 41. Sample capacitance versus exposure time for control and coupling agent modified composite samples tested to expose fiber ends



**Table X. Calculated Debonded Area for End-On EIS Measurements**

<b>Fiber Finish</b>	<b>Exposure Time (hours)</b>	<b>Area at t = 0 h (cm<sup>2</sup>)</b>	<b>Area at t = exposure time (cm<sup>2</sup>)</b>
unsized	9.5	7.4	201
PH9301F	4.8*	3.5	2.2
PH9301F-1	4.7*	2.6	2.0
PH9304F	9.9	4.3	2.2
PH9305	9.3	2.1	47

The EIS results provide dramatic evidence of the improvement in resistance to galvanic corrosion provided by the reactive finishes. When optimized, these finishes should add only \$1-3 per pound to the cost of BMI matrix composites. As such, this approach should provide a cost-effective means of reducing the susceptibility of carbon/BMI composites to galvanic corrosion.

## **SUMMARY AND CONCLUSIONS**

This study was undertaken to improve the galvanic corrosion resistance of carbon/BMI composites through the use of a phenolic finish. In this process, each fiber is coated uniformly with the phenolic finish and bonded to the finish with reactive coupling agents before the BMI prepregging process. The finish serves to isolate the carbon fibers from the BMI matrix and interrupts the galvanic cell. Results show that this approach is a viable means of improving galvanic corrosion resistance of carbon/BMI composites and that composite mechanical properties are not compromised by the finish. Both static galvanic couples and dynamic electrochemical impedance spectroscopy measurements show that all but one of the four finishes examined dramatically improve composite corrosion resistance. Longitudinal flexure and short beam shear strength measurements show that BMI matrix composites with finished fibers are equivalent to those with unsized fibers. The mechanical data is supported by VCXPS measurements and SEM failure surface analysis that show that interfacial adhesion is superior in the finished composites. This approach will provide a cost efficient means of improving galvanic corrosion resistance in composites with any BMI formulation.



## ACKNOWLEDGMENTS

The authors would like to express their gratitude to Dr. Rob Sorenson and Dr. Rudy Buckheit at Sandia National Laboratories for conducting the electrochemical impedance spectroscopy measurements and Dr. Jim Miller at Amoco Performance Products for conducting the VC-XPS measurements. We would also like to thank Mr. Roland Cochran and Mr. Kevin Miller at the Naval Air Warfare Center for their insights during the course of the program.

## REFERENCES

1. M. C. Faudree, "Relationship of Graphite/Polyimide Composites to Galvanic Processes," Proc. 36th International SAMPE Symposium, April 1991, Society for the Advancement of Material and Process Engineering, Covina, CA, pp. 1273-87.
2. R. C. Cochran, T. M. Donnellan, and R. E. Trabocco, "Environmental Degradation of High Temperature Composites," Proc. 73rd AGARD Structures and Materials Panel, San Diego, CA, Oct. 1991, Report AGARD-R-785, April 1992, North Atlantic Treaty Organization, Neuilly sur Seine, France.
3. F. D. Wall, S. R. Taylor, and G. L. Cahen, "The Simulation and Detection of Electrochemical Damage in BMI/Graphite Fiber Composites Using Electrochemical Impedance Spectroscopy," ASTM-STP-1174, *High Temperature and Environmental Effects on Polymeric Composites*, C. E. Harris and T. S. Gates, Eds., American Society for Testing and Materials, Philadelphia, PA, 1993, pp. 95-113.
4. M. L. Rommel, A. S. Postyn, and T. A. Dyer, "Accelerating Factors in Galvanically Induced Polyimide Degradation," SAMPE J., 29, 2, Mar.-Apr. 1993, Society for the Advancement of Material and Process Engineering, Covina, CA, pp. 19-24
5. D.W. Leedy and D.L. Muck, "Cathodic Reduction of Phthalimide Systems in Nonaqueous Solutions," J. of the American Chemical Society, 93, 17, 1971, pp. 4264-4270.
6. Z. Horii, C. Iwata, and Y. Tamura, "Reduction of Phthalimides with Sodium Borohydride," J. of Organic Chemistry, 26, 1961, pp. 2273-2276.
7. R. T. Morrison and R. N. Boyd, *Organic Chemistry*, Allyn and Bacon Inc., Boston, MA, 1973, pp. 741, 888.
8. R. Taylor, AEROMAT 91, American Society for Materials, Materials Park, OH, May 1991.



9. J. Boyd, S. Speak, and P. Sheahan, "Galvanic Corrosion Effects on Carbon Fiber Composites: Results from Accelerated Tests," 37th International SAMPE Symposium, March 1992, Society for the Advancement of Material and Process Engineering, Covina, CA, pp. 1184-1198.
10. R. C. Cochran, R. E. Trabocco, J. Boodey, J. Thompson, and T. M. Donnellan, "Degradation of Imide Based Composites," 36th International SAMPE Symposium, April 1991, Society for the Advancement of Material and Process Engineering, Covina, CA, pp. 1273-1287.
11. R. C. Cochran, T. M. Donnellan, and R. E. Trabocco, "Degradation of Imide Based Composites," Proc. First Int'l Symp. on Environmental Effects on Advanced Materials (ADVMAT/91), San Diego, CA, June 1991, National Association of Corrosion Engineers, Houston TX, 1992.
12. S. Wang and A. Garton, *Proc. American Chemical Society, Polymeric Materials Science and Engineering Division*, 62, 1990, pp. 900-902.
13. L. T. Drzal, M. J. Rich, M. F. Koenig and P. F. Floyd, *J. Adhesion*, 16, 1983, pp. 133-152.
14. J. G. Williams, M. E. Donnellan, M. E. Janes and W. L. Morris, *Interfaces in Composites*, C. G. Patano and E. J. Chen, Eds., Materials Research Society, Pittsburg, PA, 170, 1989, pp. 285-290.
15. B. Okhuysen, R. C. Cochran, R. E. Allred, R. Sposilli and T. M. Donnellan, "Interface/Interphase Studies on Epoxy Matrix Composites," Proc. Int'l Symp. on The Interphase," February 21-26, 1993, Williamsburg, VA, The Adhesion Society, in press.
16. F. J. McGarry and J. E. Moalli, *SAMPE Quarterly*, 23, 4 (1992), pp. 35-38.
17. S. H. Jao and F. J. McGarry, *J. Reinforced Plastics and Composites*, 11 (1992), pp. 811-832.
18. J. Chang, J. P. Bell and R. Joseph, *SAMPE Quarterly*, 18, 3 (1987), pp. 39-45.
19. M. Labronici and H. Ishida, *Proc. 4th Int'l Conf. Composite Interfaces*, 1992, p. 33.
20. J. D. Miller, W. C. Harris, and G. W. Zajac, "Composite Interface Analysis Using Voltage Contrast XPS," *Surface and Interface Analysis*, Vol. 20, 1993, pp. 977-983.





21. J. D. Miller, R. A. Gray, D. Ward, J. B. Barr and W. C. Harris, "Relating Thermo-Mechanical Performance to Carbon Fiber/Matrix Adhesion in PMR-15 Laminates," *Proc. High Temple Workshop XIII*, 1993.
22. J. Miller, G. Zajac, and T. Nguyen, "Interlaboratory Study of Fiber/Matrix Adhesion Using Voltage Contrast XPS," *Fiber, Matrix and Interface Properties; Second Volume*, ASTM STP 1290, C. J. Spragg and L. T. Drzal, eds., Am. Chem. Soc. for Testing and Materials, 1996, pp. 92-102.
23. M.P. Stevens, *Polymer Chemistry An Introduction*, Addison-Wesley Publishing Company, Reading, MA, 1975.

DISTRIBUTION:

NAVAIRWARCENACDIV Patuxent River, MD (4.3.4.3)	(8)
NAVAIRWARCENACDIV Patuxent River, MD (Technical Publishing Team)	(1)
DTIC	(1)